

# Journal Pre-proof

Gliadin Nanoparticles Induce Immune Tolerance to Gliadin in Mouse Models of Celiac Disease

Tobias L. Freitag, Joseph R. Podojil, Ryan M. Pearson, Frank J. Fokta, Cecilia Sahl, Marcel Messing, Leif C. Andersson, Katarzyna Leskinen, Päivi Saavalainen, Lisa I. Hoover, Kelly Huang, Deborah Phippard, Sanaz Maleki, Nicholas J.C. King, Lonnie D. Shea, Stephen D. Miller, Seppo K. Meri, Daniel R. Getts

PII: S0016-5085(20)30157-8  
DOI: <https://doi.org/10.1053/j.gastro.2020.01.045>  
Reference: YGAST 63187

To appear in: *Gastroenterology*  
Accepted Date: 27 January 2020

Please cite this article as: Freitag TL, Podojil JR, Pearson RM, Fokta FJ, Sahl C, Messing M, Andersson LC, Leskinen K, Saavalainen P, Hoover LI, Huang K, Phippard D, Maleki S, King NJC, Shea LD, Miller SD, Meri SK, Getts DR, Gliadin Nanoparticles Induce Immune Tolerance to Gliadin in Mouse Models of Celiac Disease *Gastroenterology* (2020), doi: <https://doi.org/10.1053/j.gastro.2020.01.045>.

This is a PDF file of an article that has undergone enhancements after acceptance, such as the addition of a cover page and metadata, and formatting for readability, but it is not yet the definitive version of record. This version will undergo additional copyediting, typesetting and review before it is published in its final form, but we are providing this version to give early visibility of the article. Please note that, during the production process, errors may be discovered which could affect the content, and all legal disclaimers that apply to the journal pertain.

© 2020 by the AGA Institute



## **Gliadin Nanoparticles Induce Immune Tolerance to Gliadin in Mouse Models of Celiac Disease**

**Tobias L. Freitag**<sup>1,2,#</sup>, **Joseph R. Podojil**<sup>3,4</sup>, Ryan M. Pearson<sup>4,5</sup>, Frank J. Fokta<sup>4</sup>, Cecilia Sahl<sup>1</sup>,  
Marcel Messing<sup>1,2</sup>, Leif C. Andersson<sup>6</sup>, Katarzyna Leskinen<sup>2</sup>, Päivi Saavalainen<sup>2</sup>, Lisa I.  
Hoover<sup>7</sup>, Kelly Huang<sup>7</sup>, Deborah Phippard<sup>7</sup>, Sanaz Maleki<sup>8</sup>, Nicholas J.C. King<sup>8</sup>, Lonnie D.  
Shea<sup>5</sup>, Stephen D. Miller<sup>3,9</sup>, Seppo K. Meri<sup>1,2</sup>, Daniel R. Getts<sup>3,4,8,9</sup>

<sup>1</sup> Department of Bacteriology and Immunology, <sup>2</sup> Translational Immunology Research Program,  
<sup>6</sup> Department of Pathology, University of Helsinki, Finland; <sup>3</sup> Department of Microbiology and  
Immunology, <sup>9</sup> Interdepartmental Immunobiology Center, Feinberg School of Medicine,  
Northwestern University, Chicago, IL, USA; <sup>8</sup> Discipline of Pathology, School of Medical  
Sciences, Bosch Institute, Sydney Medical School, The University of Sydney, Sydney, Australia;  
<sup>5</sup> Department of Biomedical Engineering, University of Michigan, Ann Arbor, MI, USA; <sup>7</sup> Precision  
for Medicine, Frederick, MD, USA; <sup>4</sup> Cour Pharmaceutical Development Company, Northbrook,  
IL, USA

# Corresponding author

Author names in bold designate shared co-first authorship

Address Correspondence to:

Tobias L. Freitag, MD  
Translational Immunology Research Program  
Department of Bacteriology and Immunology  
Haartmaninkatu 3, Room B327  
00290 University of Helsinki  
Finland  
eMail: tobias.freitag@helsinki.fi

### **Disclosure:**

N.J.C.K, S.D.M, L.D.S and D.R.G are shareholders of Cour Pharmaceutical Development Company. N.J.C.K, S.D.M, L.D.S and D.R.G are inventors on patent applications describing TIMP-GLIA. Based on an agreement between the University of Helsinki and Cour Pharmaceuticals Development Company, T.L.F. received funding to conduct experiments. The other authors have no financial arrangements to disclose.

**Author contributions:**

T.L.F., N.J.C.K., J.R.P., S.D.M., S.K.M. and D.R.G. planned the study and experiments. T.L.F., J.R.P., R.M.P., F.J.F., C.S., M.M., K.L., S.K., L.I.H, K.H. and S.M. performed experiments. T.L.F., J.R.P., C.S., L.C.A., K.L., P.S., L.I.H., N.J.C.K., L.D.S., S.D.M., S.K.M. and D.R.G. analyzed and interpreted results. T.L.F. and D.R.G. drafted and N.J.C.K., L.D.S., S.D.M. and S.K.M. edited the manuscript.

**Acknowledgements**

This study was performed with funding by Cour Pharmaceuticals Development, Inc., National Health and Medical Research Council grant 1030897 (to D.R.G and N.J.C.K), National Institutes of Health Grant EB-013198 (to S.D.M), Helsinki University Central Hospital (TYH2014307) and Academy of Finland (292393) grants (both to S.K.M).

We thank Mari Rissanen (Centre for Drug Research, University of Helsinki) for technical assistance with mouse intravenous injections, and Ulla Kiiski and Leena Saikko (both at the Dept. of Pathology, University of Helsinki) for technical assistance with histology and immunohistochemistry, respectively.

**Study approval.** Human blood cell and plasma samples were provided by Precision for Medicine (Frederick, MD, USA) and BTS Research (San Diego, CA, USA). Precision for Medicine and BTS Research obtained approvals from their respective institutional review boards for all the studies reported. Informed consent was obtained from all participants. All animal procedures were approved by the Northwestern University Institutional Animal Care and Use Committee (A3283-01), or the Southern Finnish State Administrative Agency (ESAVI/1064/04.10.03/2012 and ESAVI/1286/04.10.07/2016).

**Abbreviations**

Antigen (Ag), antigen-presenting cells (APC), complete Freund's adjuvant (CFA), delayed-type hypersensitivity (DTH), dendritic cells (DC), gluten-free diet (GFD), granulocyte-macrophage colony-stimulating factor (GM-CSF), human equivalent dose (HED), human leukocyte antigen (HLA), interferon gamma (IFNG), interleukin 2 (IL2), interleukin 4 (IL4), interleukin 10 (IL10), interleukin 17 (IL17), macrophage receptor with collagenous structure (MARCO), multiple sclerosis (MS), peripheral blood mononuclear cells (PBMC), poly(ethylene-alt-maleic acid) (PEMA), poly(lactide-co-glycolide) (PLGA), poly(vinyl acetate) (PVA), T-helper 1 (Th1) cell, T-helper 17 (Th17) cell, transforming growth factor beta (TGFB), T-regulatory cells (Treg cells), sodium dodecyl sulfate polyacrylamide gel electrophoresis (SDS-PAGE), standard deviation (SD), standard error of the mean (SEM), tolerogenic immune-modifying nanoparticles (TIMP), tolerogenic immune-modifying nanoparticles containing gliadin (TIMP-GLIA), type 1 diabetes (T1D).

**Abstract:**

**Background & Aims:** Celiac disease could be treated, and potentially cured, by restoring T-cell tolerance to gliadin. We investigated the safety and efficacy of negatively charged, 500 nm, poly(lactide-co-glycolide) nanoparticles encapsulating gliadin protein (TIMP-GLIA) in 3 mouse models of celiac disease. Uptake of these nanoparticles by antigen-presenting cells was shown to induce immune tolerance in other animal models of autoimmune disease.

**Methods:** We performed studies with C57BL/6, RAG1<sup>-/-</sup> (C57BL/6), and HLA-DQ8, huCD4 transgenic Ab0 NOD mice. Mice were given 1 or 2 tail-vein injections of TIMP-GLIA or control nanoparticles. Some mice were given intradermal injections of gliadin in complete Freund's adjuvant (immunization), or of soluble gliadin or ovalbumin (ear challenge). RAG1<sup>-/-</sup> mice were given intraperitoneal injections of CD4<sup>+</sup>CD62L<sup>-</sup>CD44<sup>hi</sup> T cells from gliadin-immunized C57BL/6 mice, and were fed with AIN-76A-based diet containing wheat gluten (oral challenge), or without gluten. Spleen or lymph node cells were analyzed in proliferation and cytokine secretion assays, or by flow cytometry, RNA sequencing or real-time quantitative PCR. Serum samples were analyzed by gliadin antibody ELISA, and intestinal tissues were analyzed by histology. Human PBMC, or immature dendritic cells derived from human PBMC, were cultured in medium containing TIMP-GLIA, anti-CD3 antibody, or LPS (controls) and analyzed in proliferation and cytokine secretion assays or by flow cytometry. Whole blood or plasma from healthy volunteers was incubated with TIMP-GLIA, and hemolysis, platelet activation and aggregation, and complement activation or coagulation were analyzed.

**Results:** TIMP-GLIA did not increase markers of maturation on cultured human dendritic cells or induce activation of T cells from patients with active or treated celiac disease. In the delayed-type hypersensitivity (model 1), the HLA-DQ8 transgenic (model 2), and the gliadin memory T cell enteropathy (model 3) models of celiac disease, intravenous injections of TIMP-GLIA significantly decreased gliadin-specific T cell proliferation (in models 1 and 2), inflammatory cytokine secretion (in models 1, 2, and 3), circulating gliadin-specific IgG/IgG2c (in models 1 and 2), ear swelling (in model 1), gluten-dependent enteropathy (in model 3), and body weight loss (in model 3). In model 1, the effects were shown to be dose dependent. Splenocytes from HLA-DQ8 transgenic mice given TIMP-GLIA nanoparticles, but not control nanoparticles, had increased levels of FOXP3, and gene expression signatures associated with tolerance induction.

**Conclusions:** In mice with gliadin sensitivity, injection of TIMP-GLIA nanoparticles induced unresponsiveness to gliadin, and reduced markers of inflammation and enteropathy. This strategy might be developed for treatment of celiac disease.

**Keywords:** Gluten sensitivity, tolerogenic vaccine, immunotherapy, immunomodulation

## Introduction

Celiac disease is a gluten-sensitive enteropathy with a prevalence of 0.3-2.4% in most populations. Celiac disease results from the failed immune regulation of gluten-specific CD4+ T cells in individuals carrying human leukocyte antigen (HLA)-DQ2 or HLA-DQ8 risk alleles.<sup>1</sup> In celiac disease patients, exposure to gluten leads to the activation of gluten-specific-T cells, culminating in immune-mediated intestinal damage.<sup>2</sup> Therapeutic approaches that render T cells tolerant to gluten have the potential to cure celiac disease. The induction of sustained unresponsiveness to gluten could eliminate the life-time burden of dietary restriction, clinical symptoms associated with accidental gluten exposure, and the risk of severe long-term complications, such as malignancies, secondary autoimmune diseases or bone loss.<sup>3</sup> However, until now no attempt to induce tolerance in autoimmune disease patients has shown clinical efficacy.

Recently, we demonstrated the tolerogenic potential of antigen loaded, negatively charged nanoparticles (referred to as Tolerogenic Immune Modifying Nanoparticles, TIMP) in murine models of multiple sclerosis (MS), transplantation, airway allergy, and type 1 diabetes (T1D).<sup>4,5,6,7</sup> Previous studies have shown that TIMP, when injected intravenously, are mainly directed to the spleen and the liver.<sup>8,9,10</sup> In these organs, tissue-resident antigen presenting cells (APC), including splenic marginal zone macrophages expressing macrophage receptor with collagenous structure (MARCO), take up TIMP.<sup>8,9,10,11</sup> A recent mechanistic study demonstrated uptake of TIMP by both macrophages and dendritic cells, TIMP localization to endolysosomes, altered APC transcriptional activity following TIMP uptake, upregulation of surface MHC class II

presentation of specific peptide, and induced downregulation of co-stimulatory molecules CD80 and CD86 on the surface of APC.<sup>12</sup> Studies using nanoparticles or apoptotic cells have shown that treatment resulted in the upregulation of inhibitory ligands on macrophages, such as PD-L1, and the production of regulatory cytokines, such as interleukin 10 (IL10) and transforming growth factor beta (TGFB), in the spleen.<sup>7,13,14</sup> Additionally, these antigen-specific therapies induced CD4+ T cell anergy, and the activation of CD4+ T-regulatory (Treg) cells.<sup>4,7,13,14</sup> The overall result was a decrease in pro-inflammatory CD4+ and CD8+ T cell activity, reduction in leukocyte accumulation in tissues, and decreased clinical signs of disease.

Based on these observations, we hypothesized that intravenous administration of gliadin protein encapsulated in TIMP (referred to as TIMP-GLIA), harboring immunodominant and subdominant gliadin epitopes<sup>15,16</sup>, may restore peripheral tolerance to gluten. Here, we report results of the generation and subsequent preclinical evaluation of TIMP-GLIA, produced to good-manufacturing practices, and currently being tested in human phase 1/2 clinical trials. Administration of TIMP-GLIA proved highly effective at inducing gliadin immune tolerance and reduction of gliadin-specific inflammatory responses, including gluten enteropathy, in three rodent models of celiac disease. Previously identified gene targets of TIMP were confirmed, and several novel targets identified. Additional studies showed that TIMP-GLIA were biocompatible in human blood.



## Materials and Methods

### Particle synthesis

PLGA particles encapsulating gliadin from wheat (Sigma-Aldrich, St. Louis, MO) were fabricated using a double emulsion technique, by first dissolving 400 mg of PLGA (Lactel Absorbable Polymers, Birmingham, AL) in 2 mL of ethyl acetate. Subsequently, 10 mg of gliadin was dissolved at 25 mg/ml in 0.05 M acetic acid, and added to the PLGA solution. The solution was emulsified by sonication for 30s at 100% amplitude using a Cole-Parmer CPX130 Ultrasonic Processor, equipped with a Cole-Parmer CV 18 ultrasonic probe adapter and a Cole-Parmer 3 mm probe with stepped tip. Immediately after sonication, 10 ml of 1% w/v poly(ethylene-alt-maleic anhydride) (PEMA) or 2% poly(vinyl alcohol) (PVA; both from Polysciences, Warrington, PA) was poured into the first emulsion, and sonicated for an additional 30s at 100% amplitude. Following the second sonication, the emulsion was poured into 200 ml 0.5% PEMA or 0.5% PVA, and was stirred overnight to remove residual organic solvents. The nanoparticles were then washed three times in 0.1 M sodium carbonate-sodium bicarbonate buffer, pH 9.6. The nanoparticles were then resuspended in 20 ml 3% w/v aqueous D-mannitol and 4% w/v aqueous sucrose, frozen in liquid nitrogen, lyophilized and stored for future use. The amount of protein encapsulated were determined from nanoparticles dissolved in DMSO, using the CBQCA Protein assay (Molecular Probes, Waltham, MA). PLGA nanoparticles encapsulating Cy5.5 dye, ovalbumin or lysozyme were prepared as previously described.<sup>4,6</sup>

## Animals

C57BL/6, RAG1<sup>-/-</sup> (C57BL/6) and HLA-DQ8, huCD4 transgenic Ab0 NOD mice<sup>17</sup> were purchased from The Jackson Laboratory, Bar Harbor, ME. All mice were housed under specific pathogen-free conditions in the Northwestern University Center for Comparative Medicine, or the University of Helsinki Laboratory Animal Centre, and were raised on normal chow, or gluten-free, standardized diet (AIN-76A; Research Diets, New Brunswick, NJ), as indicated. Some groups of mice were challenged with AIN-76A-based diet containing 2.5 g wheat gluten/kg (Sigma Aldrich; prepared by Research Diets). To compare the effects of different treatments, some groups of mice were injected one or two times into the tail vein with TIMP-GLIA, control nanoparticles containing lysozyme (TIMP-LYS), ovalbumin (TIMP-OVA) or unloaded (TIMP; nanoparticle dose range 0.025-2.5mg, time points as indicated; each in 200µl of PBS), or 25-40µg soluble gliadin in 200µl of PBS.

## Gliadin delayed-type hypersensitivity (DTH) model

Female C57BL/6 mice (6-7 weeks old) were immunized subcutaneously with 100µl of an emulsion containing 200µg of *M. tuberculosis* H37Ra (BD Biosciences, San Jose, CA) and 100µg of gliadin, distributed over three sites on the flank. Gliadin (SAFC, Madison, WI) was reconstituted from lyophilized powder in 50mM acetic acid (5 mg/ml). This gliadin solution was then further diluted for use in PBS. Mice were treated intravenously with different nanoparticle preparations, on days -7, 0 or 7, as indicated.

On day 14 after priming, mice were bled, and tested for delayed type hypersensitivity (DTH). Mice were anaesthetized by inhalation of isoflurane, and baseline pinna thickness was measured for both ears using calipers (Mitutoyo Thickness Gage; Global Industrial, Port Washington, NY). Immediately following pinna thickness assessments, using a Hamilton syringe with a 30G1/2 needle, gliadin or negative control OVA protein (10 $\mu$ l at 1mg/ml) in PBS was intradermally injected into the left and right ear, respectively. The increase in ear thickness was determined after 24h, and the change in pinna thickness ( $\Delta T$ ) was calculated using the following equation: ( $\Delta T = (\text{pinna thickness at 24hrs following elicitation}) - (\text{pinna thickness prior to elicitation})$ ). Mice were then sacrificed, and cell suspensions from draining lymph nodes or spleens were prepared.

#### **HLA-DQ8 transgenic mouse model**

2 groups of female HLA-DQ8 mice were treated intravenously on days -11 and -3 with TIMP-GLIA, or TIMP-OVA, while 2 other groups remained without treatment (2.5mg/dose; n=11-19, 10-12 weeks of age, raised on gluten-free diet AIN-76A). On day 0, mice from both the TIMP-GLIA, the TIMP-OVA and 1 control group of mice (IMMU ONLY) were injected at the base of the tail with 100  $\mu$ g gliadin in complete Freund's adjuvant, followed by 50  $\mu$ g gliadin in incomplete Freund's adjuvant on day 14 (Sigma-Aldrich). The second control group (NO TREATMENT) remained untreated. On days 28-30, mice were anesthetized with ketamine/xylazine. Blood was collected retro-orbitally, and serum stored at -20°C. Spleens were harvested for analyses.

**Gliadin Memory T cell Enteropathy Model.** Male C57BL/6 donor mice, raised on gluten-free diet AIN-76A, were injected at the base of the tail with 100 µg gliadin in complete Freund's adjuvant, followed by 50 µg gliadin in incomplete Freund's adjuvant after 2 weeks (Sigma-Aldrich). CD3<sup>+</sup> T cells were isolated after 4-5 weeks from spleen cell suspensions, using antibody-coated columns. Memory CD4<sup>+</sup> T cells were isolated from CD3<sup>+</sup> T cells using CD4<sup>+</sup>CD62L<sup>+</sup>CD44<sup>hi</sup> T cell columns, as reported (both columns from R&D Systems, Minneapolis, MN).<sup>18,19</sup> Four groups of male Rag1<sup>-/-</sup> mice (n=16, 6-10 weeks of age, matched for body weight) were injected intraperitoneally on day 0 with  $3 \times 10^5$  splenic CD4<sup>+</sup>CD62L<sup>+</sup>CD44<sup>hi</sup> T cells. Recipient mice were challenged until the end of the experiment with AIN-76A-based diets containing 2.5 g wheat gluten/kg, or no gluten added. Mice from 2 groups were either injected into the tail vein with TIMP-GLIA (2.5mg dose, in 200µl of PBS), or with 2.5mg of TIMP-LYS (nanoparticle treatment control), both on day 10 and 24. Mice were monitored and body weights were recorded for 8 weeks after adoptive transfers, and then mice were sacrificed for organ harvest.

## Statistics

RNA sequencing data were analyzed with edgeR.<sup>20</sup> Other data were analyzed with Prism 8 software (GraphPad, La Jolla, CA). Statistical comparisons were performed using paired or unpaired Student's *t*-tests, *t*-tests corrected for multiple testing using the Holm-Sidak method (alpha=0.05), one-way ANOVA and Tukey's tests for comparisons

between multiple groups, or Kruskal-Wallis and Dunn's tests for nonparametric data, as indicated. Means, medians, SD, SEM and interquartile ranges were calculated.

## Results

### **Development of Tolerogenic Immune-Modifying Nanoparticles encapsulating gliadin extracted from wheat (TIMP-GLIA)**

Previous studies have demonstrated the importance of negative charge in nanoparticle tolerance induction.<sup>21</sup> Therefore, we tested the potential for poly(lactide-co-glycolide) (PLGA) nanoparticles with different zeta potentials to be taken up by macrophages, and for inducing immune tolerance in a gliadin-specific delayed-type hypersensitivity (DTH) model. Different formulations were prepared, using a double emulsion-solvent evaporation, and either poly(ethylene-alt-maleic acid) (PEMA) as the stabilizing anionic surfactant, or poly(vinyl acetate) (PVA) as the neutral stabilizing surfactant. Particles encapsulated either the fluorescent dye Cy5.5, gliadin isolated from wheat, ovalbumin or no dye/protein (Fig 1A). PLGA-PEMA-Cy5.5 nanoparticles with high negative zeta potential (approx. -40 mV) interacted strongly with bone marrow-derived macrophages, whereas PLGA-PVA-Cy5.5 nanoparticles with a more neutral zeta potential (approx. -20 mV) did not reach the same levels (Fig 1B). Correspondingly, in a gliadin DTH mouse model, intravenous treatment on days 0 and 7 with two injections of 2.5 mg/mouse PLGA-PEMA-GLIA following gliadin/CFA priming was associated with significant decreases in ear swelling when compared to control animals receiving either PLGA-PVA-GLIA, or PLGA-PEMA-OVA (Fig 1C). This result was similar to our previous findings<sup>8,21</sup>, demonstrating that nanoparticles with higher negative

charge showed increased efficacy in reducing ear swelling in DTH models. Furthermore, the importance of nanoparticle encapsulation of protein was also confirmed, as the intravenous injection of 25 µg soluble (free) gliadin alone did not show any efficacy in reducing ear swelling in the gliadin DTH model (Fig 1D).

Based on this experience, PLGA-PEMA nanoparticles encapsulating gliadin were prepared (now referred to as TIMP-GLIA; structure shown schematically in Fig 2A). Nanoparticles containing no protein, ovalbumin (TIMP-OVA), or lysozyme (TIMP-LYS) were synthesized as control particles (Fig 2B).<sup>6,8</sup> The loading of TIMP with gliadin was controlled by adjusting the concentration of gliadin during formulation, and was aimed at  $10 \pm 5$  µg protein per mg of PLGA. To determine whether TIMP-GLIA or TIMP-OVA displayed antigen on the particle surface, surface protein binding of antigen-specific antibodies was measured by FACS. Less than 1% of TIMP were found to be positive for surface protein. Sodium dodecyl sulfate polyacrylamide gel electrophoresis (SDS-PAGE) and Western Blot confirmed the presence of gliadin  $\alpha/\beta$ ,  $\gamma$  and  $\omega$  proteins in TIMP-GLIA (Fig 2C; Supplementary Fig 1). Scanning electron microscopy of TIMP-GLIA suspensions confirmed the size and a spherical morphology with a smooth surface (Fig 2D). Additionally, in use stability testing showed that reconstituted TIMP-GLIA remained stable for up to at least 8 hours after rehydration, with burst release, average size and zeta potential remaining unchanged during this time (Fig 2E-G).

**TIMP-GLIA tolerance induction in mice with delayed-type hypersensitivity to gliadin is dose-dependent, and effective when given before or after gliadin immunization.**

To analyze further the efficacy and specificity of TIMP-GLIA tolerance induction, we pre-treated mice on days -7 and day 0 in the DTH model. Intravenous pre-treatment with two injections of 0.025 mg - 2.5 mg/mouse (1.25 - 125 mg/kg) TIMP-GLIA prior to gliadin/CFA priming was not associated with any clinical symptoms or adverse events in mice. While pre-treatment with 0.025 mg/mouse (1.25 mg/kg) failed to show efficacy, doses of 0.25-2.5 mg/mouse (12.5-125 mg/kg) TIMP-GLIA were associated with significant decreases ( $p < 0.0001$ ) in ear swelling when compared to control animals receiving unloaded nanoparticles (IMP; Fig 3A). Immediately after measuring ear swelling, the spleens were collected and the CD4<sup>+</sup> T cell populations present within the spleen examined by flow cytometry. The spleens of animals that had received two infusions of TIMP-GLIA had significantly reduced numbers of proliferating, interferon gamma (IFNG)-producing CD4<sup>+</sup> effector T cells in the spleen, as determined by intracellular cytokine staining (Fig 3B; gating strategy in Supplementary Fig 2). The decrease in effector T cells observed in TIMP-GLIA treated animals correlated with a dose-dependent reduction in T cell proliferation (Fig 3C) in splenocyte cultures when restimulated with gliadin. Therefore, pre-treatment of mice with TIMP-GLIA prior to gliadin/CFA immunization induced a tolerogenic phenotype in gliadin-specific CD4<sup>+</sup> T cells. Furthermore, this phenotype appeared to result in reduced T cell help, required for anti-gliadin antibody production, as treatment with 2.5mg/mouse TIMP-GLIA resulted in significant reduction in circulating levels of gliadin-specific IgG (Fig 3D).

Subsequently, TIMP-GLIA tolerization was also tested in mice following immunization. TIMP-GLIA was administered several hours after priming (day 0), and again on day 7 after immunization. While treatment with 0.025 mg/mouse (1.25 mg/kg) failed to show efficacy, doses of 0.25-2.5 mg/mouse (12.5-125 mg/kg) were associated with significant decreases in ear swelling when compared to controls (Fig 3E). The most robust decrease in DTH was observed in animals receiving 2.5 mg/mouse (a human equivalent of 10.16 mg/kg using body surface area). Animals that had received 0.25-2.5 mg/mouse TIMP-GLIA had reduced numbers of proliferating, IFNG-producing CD4+ effector T cells in the spleen, compared to the lowest dose (Fig 3F). Gliadin recall experiments further demonstrated a dose-dependent effect. While spleen cells from animals receiving 0.025mg/mouse TIMP-GLIA showed unchanged T cell proliferation, two infusions of 0.25-2.5 mg/mouse/dose resulted in a significant inhibition of T cell proliferation (Fig 3G). Furthermore, TIMP-GLIA administration after immunization was associated with a reduction in circulating gliadin specific IgG (Fig 3H).

In an additional experiment, we tested the effects of 2.5mg TIMP-GLIA vs. IMP, administered intravenously to mice both on days 0 and 7 after gliadin immunization, on cytokine secretion of ear draining lymph node cells or spleen cells restimulated with gliadin on day 15. The results demonstrated significant reductions in inflammatory cytokines IFNG and interleukin 17 (IL17), but not in regulatory cytokine IL10, in mice treated with TIMP-GLIA (Supplementary Fig 3A-F). Taken together, the data obtained in the DTH model showed that TIMP-GLIA induced gliadin-specific tolerance in a dose-dependent fashion even in the context of a robustly activated immune response, without causing any apparent adverse effects.



## **TIMP-GLIA tolerance induction in transgenic mice expressing celiac disease-associated HLA-DQ8**

To address the potential of TIMP-GLIA to induce tolerance in the context of the human leukocyte antigen DQ8 risk allele (HLA-DQ8) associated with celiac disease, Ab0 NOD mice (mouse MHC II deficient) expressing HLA-DQ8 and human CD4 transgenes were used.<sup>15</sup> These mice, raised and maintained on a gluten free diet and subsequently immunized with gliadin/CFA, develop gliadin-specific B cell and CD4+ T cell responses. In this study, treatment of HLA-DQ8 mice with 2.5 mg/mouse (125 mg/kg) TIMP-GLIA or TIMP-OVA control on days -11 and -3 prior to immunization with gliadin/CFA (Fig 4A), did not appear to alter the levels of circulating anti-gliadin IgG1 (Supplementary Fig 4), but reduced the amount of T-helper 1 (Th1) cell-associated, complement-fixing anti-gliadin IgG2c, compared to TIMP-OVA control-treated mice (Fig 4B). In addition, TIMP-GLIA treatment resulted in significant reductions of T cell proliferation (Fig 4C) and inflammatory cytokine secretion in response to gliadin restimulation of splenocytes (IFNG, IL17; Fig 4D, E). While only non-significant reductions were observed for interleukin 2 (IL2) and the regulatory cytokine IL10 (Fig 4F, G), TIMP-GLIA treatment increased regulatory T cell specific forkhead box P3 (Foxp3) mRNA expression by gliadin-restimulated splenocytes in RT-qPCR (resulting in significant reductions of  $\Delta$ CT values vs. TIMP-OVA, Fig 4H). Together, these results demonstrate gliadin-specific tolerance induction by TIMP-GLIA in HLA-DQ8 mice, and the involvement of FOXP3+ Tregs in the modulation of the gliadin recall response.

To further characterize mechanistic pathways involved in TIMP-GLIA tolerance induction, we performed RNA sequencing of gliadin-restimulated splenocytes from three

groups of treated HLA-DQ8 mice (TIMP-GLIA, TIMP-OVA, IMMU ONLY; Fig 4A), more than four weeks after the last dose of TIMP-GLIA had been administered. We found 77 genes differentially expressed, either between TIMP-GLIA vs. TIMP-OVA treated mice, or TIMP-GLIA vs. IMMU ONLY (Supplementary Fig 5). Of these, 15 genes showed significant differences in both comparisons, thus reconfirming results. A comparison between TIMP-OVA and IMMU ONLY did not reveal any differentially expressed genes, supporting an antigen-specific effect on gene regulation by TIMP-GLIA (Venn diagram, Fig 4I). The identities of these 15 genes, and their expression levels between samples from different groups, revealed long-term changes induced by TIMP-GLIA treatment in pathways of APC function (Tspan13, Cd83, Nrp2), B cell activation and differentiation (Cd79a, Ms4a1/Cd20, Ms4a4c), MHC II peptide loading (H2-DM, H2-O) and T cell cytokine secretion (Il17a, Il17f; gene expression heatmap, Fig 4J). The RNA sequence data has been deposited to NCBI Gene Expression Omnibus (Accession No.: GSE140736).

### **TIMP-GLIA tolerance induction reverses gliadin memory T cell enteropathy in mice**

Based on the robust treatment responses observed above, we determined the efficacy of TIMP-GLIA in an adoptive gliadin memory T cell transfer model of celiac disease. In contrast to the animal models above, this model mimics the gluten-dependent enteropathy characteristic of celiac disease.<sup>18,19</sup> Splenic CD4+CD62L-CD44<sup>hi</sup> memory T cells isolated from gliadin immunized C57BL/6 donor mice were transferred into four groups of male Rag1<sup>-/-</sup> mice (n=16; matched for body weight). On

the same day, three of the groups were introduced to a gluten-containing diet, while one group remained on gluten-free diet (GFD negative control). Mice from two groups on gluten-containing diet were subsequently treated on days 10 and 24 with 2.5 mg/mouse (125 mg/kg) of TIMP-GLIA i.v., or TIMP-LYS (nanoparticle treatment control), while the third group on gluten-containing diet did not receive injections with nanoparticles (GLUTEN diet positive control; Fig 5A). For statistical analysis, we combined four matched experiments, all showing similar results. As is typically seen in this model, the GLUTEN positive control group gained less body weight until week 4, and subsequently lost weight more rapidly, when compared to the GFD control. However, mice in the TIMP-GLIA group were protected from weight loss over the entire study period, similar to gluten free diet control animals. In comparison, the TIMP-LYS treatment control group lost weight, and did not differ significantly from GLUTEN diet control (Fig 5B). In agreement with this result, treatment with TIMP-GLIA significantly reduced the severity of histological duodenitis compared to GLUTEN positive control, while TIMP-LYS treatment did not, indicating that the effect of TIMP-GLIA on small bowel pathology was antigen-specific (Fig 5C). Duodenal sections that exemplify histological duodenitis severity scores of normal, mild, moderate or severe duodenitis are shown (Fig 5D-G; hematoxylin/eosin staining).

Consistent with results in HLA-DQ8 mice, treatment with TIMP-GLIA reduced secretion of pro-inflammatory IFNG, IL17, and IL2 cytokines by spleen cells restimulated with gliadin, compared to GLUTEN positive control or TIMP-LYS treatment control (Fig 5H-J), but not of regulatory cytokine IL10 (Fig 5K). Thus, TIMP-GLIA treatment inhibited gliadin-specific Th1/T-helper 17 (Th17) cell responses, while not

altering the IL10-mediated regulatory response. In summary, treatment with TIMP-GLIA reversed the effects of dietary gluten exposure also in this intestinal celiac disease model, similar to the effect of GFD (negative control), while control treatment with TIMP-LYS showed minor effects only. Therefore, the findings confirmed that TIMP-GLIA treatment induced a tolerogenic phenotype within the gliadin-specific T cell population.

### **TIMP-GLIA clearance and biodistribution**

To determine TIMP-GLIA circulating time, C57BL/6 mice were injected intravenously with 2.5mg TIMP-GLIA vs. 40 $\mu$ g soluble gliadin. Gliadin in plasma was quantified over 24h. The gliadin plasma concentration after injection of TIMP-GLIA peaked at 1h, rapidly declined until 4h, and had returned to baseline at 24h after injection, as determined by ELISA (Fig 6A).

### **Human peripheral blood monocyte (PBMC)-derived dendritic cells maintain an immature phenotype when treated with TIMP-GLIA, consistent with the induction of tolerance**

TIMP induced antigen-specific tolerance has been shown in rodent models to harnesses physiological systems of apoptotic cellular debris clearance and homeostasis to induce T cell non-responsiveness. To address whether TIMP-GLIA is being perceived as apoptotic by APCs, such as dendritic cells (DC), in humans, we next examined the potential for TIMP-GLIA to induce PBMC derived DC maturation, following a reference protocol. Primary cultures of human monocytes were treated with interleukin 4 (IL4) and granulocyte-macrophage colony-stimulating factor (GM-CSF) for 7 days to generate

immature DC. Maturation of DC was assessed by flow cytometry, following culture of the resultant immature DCs in the presence of TIMP-GLIA at increasing doses for 48hrs (0.008 mg/ml – 2 mg/ml). No increases in the surface expression of HLA-ABC, HLA-DR, CD14, CD83, CD80 or CD86 were observed in comparison to negative control, or immature DC that were cultured in the presence of LPS (Fig 6 B-D). Together the data show that TIMP-GLIA did not result in activation of human monocyte-derived DC, but in maintenance of low levels of co-stimulatory molecules and HLA, suggesting a tolerogenic DC phenotype.

**TIMP-GLIA shows promising human *in vitro* biocompatibility, and is non-activating when incubated with PBMC from CD patients and controls**

The induction of tolerance using the TIMP platform is contingent upon intravenous infusion. Following reference protocols, we determined the biocompatibility of TIMP-GLIA, by adding into human blood increasing doses of TIMP-GLIA, spanning the theoretical plasma concentration, calculated from the TIMP-GLIA mouse optimum/human equivalent dose (0.127mg/ml; Supplementary Fig 6A). TIMP-GLIA did not trigger hemolysis (Supplementary Fig 6B), platelet activation (Supplementary Fig 6C), platelet aggregation (Supplementary Fig 6D), or complement activation (as determined by levels of Bb plus, C4d and iC3b; Supplementary Fig 6E-G). Coagulation studies showed no abnormalities in prothrombin time (extrinsic pathway) at any concentration, whereas prolonged partial thromboplastin time (intrinsic pathway) and thrombin time (common pathway) were observed only at concentrations exceeding the

theoretical plasma concentration (Supplementary Figure 5H-J). Taken together, the findings suggest compatibility of TIMP-GLIA for intravenous infusion.

Finally, the potential of TIMP-GLIA to non-specifically activate CD3<sup>+</sup> T cells of celiac disease patients or healthy controls was analyzed (clinical data shown in Supplementary Table 2). No proliferation of PBMC was detected with increasing concentrations of TIMP-GLIA, exceeding the theoretical plasma concentration, confirming that no direct activation of blood T cells by TIMP-GLIA occurred (Fig. 6E). This was further supported by a lack of IFNG or IL2 T cell cytokine secretion (Fig. 6F, G).

## Discussion

Immune tolerance is a state of unresponsiveness of the immune system to foreign or self-antigens. The natural development of unresponsiveness to harmless stimuli from food, including gluten, is called oral tolerance. Oral tolerance to gluten is broken in celiac disease, for reasons unknown, and the re-establishment of oral tolerance to gluten is the goal of antigen-specific immunotherapy of celiac disease with TIMP-GLIA. While sustained unresponsiveness to food antigen may be achieved as a result of an intervention, as exemplified by oral immunotherapy of food allergy<sup>22</sup>, such therapies are not available for the treatment of celiac disease.

Gliadin-specific CD4+T cells of celiac disease patients secrete cytokines IFNG and IL2 in response to dietary gluten, provide T cell help to gliadin- or TG2-specific B cells for antibody production, and orchestrate the immune response in the celiac mucosa, leading to villous atrophy, crypt hyperplasia and mononuclear cell infiltration.<sup>1, 2</sup> In addition, several reports demonstrate that the CD4+ T cell cytokine IL17 is overexpressed in active celiac disease<sup>23,24</sup>, and is detected early in serum in response to gluten challenge.<sup>25</sup> There is no single experimental model that fully reflects human celiac disease.<sup>26</sup> Therefore, testing of TIMP-GLIA was performed using three different mouse models, each featuring major disease characteristics associated with human

celiac disease. The presented results demonstrate preclinical efficacy and safety supporting the clinical translation of TIMP-GLIA for the treatment of celiac disease. TIMP-GLIA inhibited the proliferation and cytokine IL2, IFNG and IL17 secretion of gliadin-stimulated T cells, while secretion of the regulatory cytokine IL10 remained unchanged. In addition, TIMP-GLIA increased Foxp3 expression by Treg cells stimulated with gliadin, decreased the anti-gliadin antibody production by B cells, and reduced gliadin-specific DTH, histological gluten-dependent enteropathy and body weight loss. Unloaded or control antigen-loaded TIMP used as treatment control did not show comparable effects. In summary, TIMP-GLIA induced gluten unresponsiveness in mice in an antigen-specific and dose-dependent fashion. If similar effects were induced by treatment of celiac disease patients with TIMP-GLIA, this might lead to unresponsiveness to oral gluten, and potentially, cure of celiac disease.

TIMP-GLIA was designed with antigenic gliadin protein that encompasses an array of gliadin-specific T cell epitopes. Importantly, not a single one of the many identified gliadin T cell peptides is recognized by more than two thirds of celiac disease patients.<sup>27</sup> Therefore, treatments aimed at restoring unresponsiveness to gliadin may need to modulate a variety of T cell clones, specific for a broad set of gliadin peptides.<sup>15,16,28</sup> Gliadin was successfully solubilized and encapsulated into PLGA nanoparticles with a zeta potential of approximately -40 mV, under current good manufacturing practices. The TIMP-GLIA treatment approach is based on harnessing the physiological propensity of 'tolerogenic' APCs to process and present peptide epitopes from intact proteins, thus avoiding gliadin peptide selection bias, and allowing APCs to present the



full spectrum of T cell epitopes from gliadin protein.

Since gliadin T cell epitopes frequently contain deamidated glutamine (glutamic acid) residues<sup>15,16,28</sup>, we note that as a result of the protein solubilization procedure in acetic acid, gliadin encapsulated in TIMP-GLIA is already partially deamidated.<sup>29</sup> Processing of TIMP-GLIA by APC, equipped with enzymes that can further deamidate glutamine residues of gliadin peptides, most importantly tissue transglutaminase (TG2)<sup>30,31</sup>, may lead to the presentation of both native and deamidated gliadin peptides. Irrespective, gliadin-specific T cells isolated from the intestine of celiac disease patients have frequently been shown to respond to both deamidated and native gliadin protein.

In this study, TIMP-GLIA was not associated with any drug-related toxicity in mice. In addition, a good laboratory practice repeat dose toxicology study was conducted in rats. This study found that TIMP-GLIA had a no observed adverse effect level of 75 mg/kg (human equivalent dose of ~12 mg/kg/day; HED), a level exceeding the HED calculated from the mouse optimum dose in our study (10.16 mg/kg/day). Further, a toxicokinetic (pK) analysis was performed in rats with increasing doses of TIMP-GLIA. This study determined that the maximum concentration and the area under the curve increased in proportion to the dose of TIMP-GLIA administered. The maximum plasma fraction was reached at 0.083 hours after dosing. The half-life of TIMP-GLIA ranged from 5.94 to 6.94 hours. In a completed, FDA-monitored phase 1 safety study of TIMP-GLIA (NCT03486990), and in a completed randomized, double-blind, placebo-controlled phase 2 trial of TIMP-GLIA (NCT03738475), no toxicity was noted in celiac disease

patients (unpublished results). Our human studies *in vitro* showed that TIMP-GLIA does not cause complement activation, hemolysis, platelet activation or aggregation, or activation/interference with coagulation at the estimated plasma concentration. Similar findings have been described for other PLGA nanoparticle formulations.<sup>32</sup> Surface characteristics, charge, and size have been identified as key factors important in limiting adverse interactions of nanoparticles with blood components and the innate immune system. Although TIMP-GLIA does not possess direct T cell targeting moieties, in this study the response by PBMCs isolated from celiac disease patients to TIMP-GLIA was also assessed. The results demonstrate that TIMP-GLIA does not lead to direct, broad T cell activation or T cell inflammatory cytokine secretion. Together these observations indicate safety of TIMP-GLIA, and its compatibility with intravenous administration.

Until now, none of the attempts to induce tolerance in human autoimmune diseases through oral, subcutaneous, or intramuscular antigen administration have led to the development of an approved drug. This has been proposed to be a result of antigen delivery to pro-inflammatory APC populations in the periphery, expressing high levels of MHC II and positive co-stimulatory molecules, which are associated with robust Th1 cell immune responses.<sup>33</sup> Induction of tolerance with intradermal injection of a solution of three immunodominant gliadin peptides has recently been attempted (NexVax2; ImmusanT, Inc.).<sup>34, 35</sup> Administration of gliadin peptides via this route triggered cytokine release, nausea and vomiting in celiac patients. Interestingly, plasma cytokine levels and treatment-emergent adverse events were diminished upon repeated intradermal administration of peptides. No evidence for unresponsiveness to dietary gluten was

demonstrated in these clinical studies. Here, we show that the targeted delivery of gliadin to apoptotic pathways in the spleen by intravenous infusion of TIMP-GLIA in mice leads to the suppression of inflammatory T and B cell responses upon gliadin recall, and the reduction of gliadin-/gluten-dependent organ pathology. Clinical efficacy, safety and durability of gliadin-specific immunotherapies remains to be demonstrated in celiac disease patients.

TIMP-GLIA size, charge, and route of administration are designed to direct gliadin to APCs within the spleen and liver. Similar PLGA particles have been shown to be taken up in a tolerogenic fashion by APCs.<sup>4,5,6,7,8,12</sup> Here we show that TIMP-GLIA at concentrations derived from mouse optimum/human equivalent doses does not trigger human monocyte-derived dendritic cell maturation, or proinflammatory pathways. In addition to these direct effects on APC, we characterized the long-term immunomodulatory signature of TIMP-GLIA. Changes in the gliadin recall response of spleen cells from tolerized HLA-DQ8 transgenic mice were identified more than four weeks after the last dose had been administered (RNAseq; RT-qPCR; cytokine ELISA). Genes modulating APC function (Tspan13, Cd83, Nrp2), MHC class II peptide presentation (H2-DM, H2-O), B cell activation/differentiation (Cd79b, Ms4a1/Cd20, Ms4a4c) and T cell differentiation/cytokine secretion (Foxp3, Ifng, Il17, Il2) were identified as directly or indirectly regulated targets, confirming earlier but more limited results using antigens coupled to apoptotic cells<sup>13,14</sup> or contained in PLGA nanoparticles.<sup>7</sup> Collectively, these results indicate that TIMP-GLIA modulates the

response of gliadin memory B and T cells, consistent with the treatment outcomes in three celiac mouse models in our study.

Interestingly, the modulation of HLA class II gliadin presentation by HLA-DM and HLA-DO has already been identified as a therapeutic opportunity in celiac disease. The celiac disease-associated risk alleles HLA-DQ2.5 and HLA-DQ8 appear to interact poorly with HLA-DM, resulting in prolonged retention of gliadin peptides, and increased effector T cell stimulation.<sup>36</sup> Increased expression of HLA-DM and/or HLA-DO in APCs, as a long-term effect of TIMP-GLIA treatment, may improve the efficiency of gliadin peptide exchange, thus inhibiting HLA-DQ2.5- and HLA-DQ8-restricted gliadin presentation.

Successful reintroduction of durable immune tolerance to gluten would represent a cure for celiac disease patients. The evidence provided here supports the ability for TIMP-GLIA to establish sustained unresponsiveness to gluten in mice, which in the context of human disease may not only alleviate the need for a gluten-free diet, but might also reduce disease complications such as secondary autoimmune diseases, bone loss or lymphoma. The therapeutic potential of TIMP-GLIA is currently under investigation in phase 1/2 clinical trials (NCT03486990 and NCT03738475).

### Figure Legends

**Figure 1: Development of Tolerogenic Immune-Modifying Nanoparticles encapsulating gliadin (TIMP-GLIA) (I).** **A)** Six different formulations of nanoparticles were prepared for testing, using either PEMA or PVA as stabilizing surfactant, and encapsulating either Cy5.5 dye, gliadin or ovalbumin (or remaining unloaded). Size, charge and protein loading were measured (mean +/- SD). **B)** PLGA-PEMA-Cy5.5 or PLGA-PVA-Cy5.5 particles were added to bone marrow-derived macrophage cultures. Cells were analyzed by flow cytometry for mean fluorescence intensity, or for percentage of Cy5.5+/DAPI- live cells (triplicates; mean +/- SD). **C)** Intravenous treatment effect of PLGA-PEMA-GLIA, PLGA-PVA-GLIA or PLGA-PEMA-OVA in the gliadin DTH mouse model. Ear thickness was measured 24h after injection of either gliadin or ovalbumin (n=5;  $\Delta$  mean ear thickness +/- SEM;  $\times 10^{-4}$ in). **D)** Treatment effect of PLGA-PEMA-GLIA, soluble gliadin or PLGA-PEMA (unloaded) in the gliadin DTH mouse model (n=5;  $\Delta$  mean ear thickness +/- SEM;  $\times 10^{-4}$ in). Statistical analyses were performed using one-way ANOVA and Tukey's multiple comparison test (**C, D**; \*p $\leq$ 0.05, \*\*p $\leq$ 0.01, \*\*\*p $\leq$ 0.001)

**Figure 2: Development of Tolerogenic Immune-Modifying Nanoparticles**

**encapsulating gliadin (TIMP-GLIA) (II).** **A)** Schematic representation of TIMP. **B)** Four different formulations of PLGA-PEMA nanoparticles were prepared for testing, encapsulating either gliadin (TIMP-GLIA), ovalbumin (TIMP-OVA) or lysozyme (TIMP-LYS), or remaining unloaded (IMP). Size, charge, protein loading (mean +/- SD) and percentage of particles positive for surface protein (FACS) were analyzed. **C)** SDS-PAGE of gliadin preparation used for production of TIMP-GLIA (duplicates, central rows). **D)** Scanning electron microscopy of a representative TIMP-GLIA suspension. **E-G)** Analysis of TIMP-GLIA stability in water over 8h, measuring protein release (**E**), size (**F**) and charge (**G**; triplicates, mean +/- SD).

**Figure 3: TIMP-GLIA tolerance induction in mice with delayed-type**

**hypersensitivity to gliadin.** **A-H)** C57BL/6 female mice (n=5) were treated with TIMP-GLIA, or unloaded control particles (IMP), either on days -7 and 0 (**A-D**), or days 0 and 7 (**E-H**). Mice were primed with gliadin in CFA on day 0. **A, E)** On day 14 post priming, mice were injected with gliadin or ovalbumin (OVA) into the ear pinna for DTH analysis ( $\Delta$  mean ear thickness after 24h +/- SEM;  $\times 10^{-4}$ in). **B, F)** The numbers of live, CD3+/CD4+/Ki67+/IFNG+ splenic effector T cells were determined (Teffs; mean +/- SEM; flow cytometry). **C, G)** To assess proliferation, spleen cells were stimulated with anti-CD3, OVA, or gliadin (mean counts per minute +/- SEM; 3H-TdR incorporation). **D, H)** Serum anti-gliadin IgG antibody levels were analyzed, testing serial dilutions (mean concentration +/- SEM; ELISA). Statistical analyses were performed using one-way

ANOVA and Tukey's multiple comparison test (**A-H**; \* $p \leq 0.05$ , \*\* $p \leq 0.01$ , \*\*\* $p \leq 0.001$ , \*\*\*\* $p \leq 0.0001$ ).

**Figure 4. TIMP-GLIA tolerance induction in transgenic mice expressing celiac disease-associated HLA-DQ8.** **A)** Experimental design. **B)** Serum anti-gliadin IgG2c antibody titers in groups of HLA-DQ8 mice, treated according to A (n=11-19; ELISA). **C)** Proliferation of spleen cells (n=8-9; BrdU ELISA). Data expressed as proliferation ratios, relating to anti-CD3/anti-CD28 positive control. **D-G)** IFNG, IL17, IL2 and IL10 cytokine concentrations in supernatants of spleen cells stimulated with gliadin, ovalbumin (negative control) or anti-CD3/anti-CD28 (positive control; n=11-19; ELISA). **H)** Foxp3 mRNA expression by spleen cells in response to gliadin restimulation (n=9-18; RT-qPCR). Results expressed in  $\Delta$ CT values (reductions of  $\Delta$ CT reflect increases in Foxp3 mRNA expression). **I)** Venn diagram depicting the numbers of genes differentially expressed in spleen cells restimulated with gliadin, in 3 separate comparisons between 3 groups of HLA-DQ8 mice (n=13-16; RNAseq). **J)** Heat map depicting the up- (red) or down-regulation (yellow) of 15 genes differentially expressed after treatment with TIMP-GLIA (n=13-16, adjusted p-value  $p \leq 0.05$ ; RNAseq). Statistical analyses were performed using one-way ANOVA and Tukey's multiple comparison test (**B, H**), t-tests corrected for multiple testing using the Holm-Sidak method (**C-G**) or edgeR (**I, J**). In plots **B-H**, significant results are indicated for comparisons between TIMP-GLIA and TIMP-OVA groups only (\* $p \leq 0.05$ , \*\* $p \leq 0.01$ ).

**Figure 5. TIMP-GLIA tolerance induction reverses gliadin memory T cell enteropathy in mice. A)** Experimental design. **B)** Total body weight development in four groups of Rag1<sup>-/-</sup> mice, treated according to A (n=14-16; data expressed as percentage of starting weight). **C)** Histological duodenitis severity scores (n=14-16; max. score 9). **D-G)** Hematoxylin/eosin staining of duodenal sections. Examples represent histological scores of **D)** 0 (normal), **E)** 3 (mild), **F)** 6 (moderate), or **G)** 9 (severe) duodenitis. Note increased villus and basal mononuclear cell infiltration, reduced villus-to-crypt ratios, and development of crypt abscesses with increasing scores. **H-K).** IFNG, IL17, IL2 and IL10 cytokine secretion in response to gliadin, or ovalbumin (Ova, negative control), in relation to anti-CD3/anti-CD28 antibody (positive control; n=9-12; ELISA; data expressed as cytokine secretion ratios). Statistical analyses were performed using one-way ANOVA and Tukey's multiple comparison test (\*p≤0.05, \*\*p≤0.01, \*\*\*p≤0.001).

**Figure 6. TIMP-GLIA clearance, and interaction with human peripheral blood mononuclear cells (PBMC). A)** Naïve C57BL/6 mice (n=3 per time point) were injected intravenously with either 2.5mg of TIMP-GLIA, or 40ug of free gliadin (corresponding amount). Mice were bled at 5min, 1h, 4h, and 24h. Collected plasma samples were assessed for the level of free gliadin (ELISA; mean concentration +/- SEM). **B-D)** Immature dendritic cells derived from human PBMC (n=6-9) were treated with vehicle (PBS), LPS 20 ng/mL (positive control) or TIMP-GLIA at increasing concentrations for 48 hours. Surface expression of HLA-ABC and HLA-DR (**B**), CD80 and CD86 (**C**) and CD14 and CD83 (**D**) were determined by flow cytometry (mean channel fluorescence;



mean  $\pm$  SD). **E-G**) Human PBMC from celiac disease patients on normal or gluten free diet, or healthy controls, were stimulated with anti-CD3 antibody (positive control) or TIMP-GLIA at increasing concentrations (triplicates; n=9-11). Proliferation (**E**), and IFNG (**F**) or IL2 (**G**) cytokine secretion were measured after 72h. Data is expressed as proliferation index (relating to unstimulated cells; luminescent cell viability assay), or cytokine concentrations (V-Plex assay). Statistical analyses were performed using paired t-test, compared to vehicle group (**B-D**; \*p $\leq$ 0.05).

## References

1. Lebwohl, B., Sanders, D.S., Green, P.H.R. Coeliac disease. *Lancet* **391**, 70-81 (2018).
2. Nilsen, E.M., Jahnsen, F.L., Lundin, K.E. et al. Gluten induces an intestinal cytokine response strongly dominated by interferon gamma in patients with celiac disease. *Gastroenterology* **115**, 551-63 (1998).
3. Anderson, R.P., Jabri, B. Vaccine against autoimmune disease: antigen-specific immunotherapy. *Curr. Opin. Immunol.* **25**, 410-7 (2013).
4. Pearson, R.M., Casey, L.M., Hughes, K.R. et al. Controlled delivery of single or multiple antigens in tolerogenic nanoparticles using peptide-polymer bioconjugates. *Mol. Ther.* **25**, 1655-1664 (2017).
5. Hlavaty, K.A., McCarthy, D.P., Saito, E. et al. Tolerance induction using nanoparticles bearing HY peptides in bone marrow transplantation. *Biomaterials* **76**, 1-10 (2016).

6. Smarr, C.B., Yap, W.T., Neef, T.P. et al. Biodegradable antigen-associated PLG nanoparticles tolerize Th2-mediated allergic airway inflammation pre- and postsensitization. *Proc. Natl. Acad. Sci. USA* **113**, 5059-64 (2016).
7. Prasad, S., Neef, T., Xu, D., Podojil, J.R. et al. Tolerogenic Ag-PLG nanoparticles induce tregs to suppress activated diabetogenic CD4 and CD8 T cells. *J. Autoimmunity* **89**, 112-124 (2018).
8. Getts, D.R., Terry, R.L., Getts, M.T., et al. Therapeutic inflammatory monocyte modulation using immune-modifying microparticles. *Sci. Transl. Med.* **6**, 219ra7 (2014).
9. McCarthy, D.P., Yap, J.W., Harp, C.T., et al. An antigen-encapsulating nanoparticle platform for T<sub>H</sub>1/17 immune tolerance therapy. *Nanomedicine* **13**, 191-200 (2017).
10. Bryant, J., Hlavaty, K.A., Zhang, X., et al. Nanoparticle delivery of donor antigens for transplant tolerance in allogeneic islet transplantation. *Biomaterials* **35**, 8887-8894 (2014).
11. Getts, D.R., Martin, A.J., Mc Carthy, D.P. et al. Microparticles bearing encephalitogenic peptides induce T-cell tolerance and ameliorate experimental autoimmune encephalomyelitis. *Nat. Biotechnol.* **30**, 1217-1224 (2012).
12. Kuo, R., Saito, E., Miller, S.D., Shea, L.D. Peptide-conjugated nanoparticles reduce positive co-stimulatory expression and T cell activity to induce tolerance. *Mol. Ther.* **25**, 1676-1685 (2017).
13. Getts, D.R., Turley, D.M., Smith, C.E. et al. Tolerance induced by apoptotic antigen-coupled leukocytes is induced by PD-L1+ and IL-10-producing splenic

- macrophages and maintained by T regulatory cells. *J. Immunol.* **187**, 2405-17 (2011).
14. Luo, X., Pothoven, K.L., McCarthy, D. et al. ECDI-fixed allogenic splenocytes induce donor-specific tolerance for long-term survival of islet transplants via two distinct mechanisms. *Proc. Natl. Acad. Sci. USA* **105**, 14527-14532 (2008).
15. Sollid, L.M., Qiao, S.-W., Anderson, R.P. et al. Nomenclature and listing of celiac disease relevant gluten T-cell epitopes restricted by HLA-DQ molecules. *Immunogenetics* **64**, 455-460 (2012).
16. Tye-Din, J.A., Stewart, J.A., Dromey, J.A. et al. Comprehensive, quantitative mapping of T cell epitopes in gluten in celiac disease. *Sci. Transl. Med.* **2**, 41ra51 (2010).
17. Hayward, S.L., Bautista-Lopez, N., Suzuki, K. et al. CD4 T cells play major effector role and CD8 T cells initiating role in spontaneous autoimmune myocarditis of HLA-DQ8 transgenic IAb knockout nonobese diabetic mice. *J. Immunol.* **176**, 7715-7725 (2006).
18. Freitag, T.L., Rietdijk, S., Junker, Y. et al. Gliadin-primed CD4<sup>+</sup>CD45RBlowCD25<sup>-</sup> T cells drive gluten-dependent small intestinal damage after adoptive transfer into lymphopenic mice. *Gut* **58**, 1597-1605 (2009).
19. Freitag, T.L., Loponen, J., Messing, M. et al. Testing safety of germinated rye sourdough in a celiac disease model based on the adoptive transfer of prolamin-primed memory T cells into lymphopenic mice. *Am. J. Physiol. Gastrointest. Liver Physiol.* **306**, G526-G534 (2014).

20. Macosko, E. Z., Basu, A., Satija, R. et al. Highly Parallel Genome-wide Expression Profiling of Individual Cells Using Nanoliter Droplets. *Cell* **161**, 1202-1214 (2015).
21. Hunter, Z., McCarthy, D.P., Yap, W.T. et al. A biodegradable nanoparticle platform for the induction of antigen-specific immune tolerance for treatment of autoimmune diseases. *ACS Nano* **8**, 2148-2160 (2014).
22. Anagnostou, K., Clark, C. What do we mean by oral tolerance? *Clin. Exp. Allergy* **46**, 782-784 (2016).
23. Monteleone, I., Sarra, M., Del Vecchio Blanco, M. et al. Characterization of IL-17A-producing cells in celiac disease mucosa. *J. Immunol.* **184**, 2211-2218 (2010).
24. Lahdenperä, A.I., Hölttä, V., Ruohtula, T. et al. Up-regulation of small intestinal interleukin-17 immunity in untreated coeliac disease but not in potential coeliac disease or in type 1 diabetes. *Clin. Exp. Immunol.* **167**, 226-234 (2012).
25. Goel, G., Daveson, A.J.M., Hooi, C.E. et al. Serum cytokines elevated during gluten-mediated cytokine release in coeliac disease. *Clin. Exp. Immunol.* **199**, 68-78 (2020).
26. Korneychuk, N., Meresse, B., Cerf-Bensussan, N. Lessons from rodent models in celiac disease. *Mucosal Immunol.* **8**, 18-28 (2015).
27. Hardy, M.Y., Girardin, A., Pizzey, C. et al. Consistency in polyclonal T-cell responses to gluten between children and adults with celiac disease. *Gastroenterology* **149**, 1541-1552.e2 (2015).

28. Vader, W., Kooy, Y., Van Veelen, P. et al. The gluten response in children with celiac disease is directed toward multiple gliadin and glutenin peptides. *Gastroenterology* **122**, 1729-1737 (2002).
29. Liao, L., Zhao, M., Ren, J. et al. Effect of acetic acid deamidation induced modification on functional and nutritional properties and confirmation of wheat gluten. *J. Sci. Food Agric.* **90**, 409-417 (2010).
30. Hodrea, J., Demeny, M.A., Majai, G. et al. Transglutaminase 2 is expressed and active on the surface of human monocyte-derived dendritic cells and macrophages. *Immunol. Lett.* **130**, 74-81 (2010).
31. Toth, B., Garabuczi, E., Sarang, Z. et al. Transglutaminase 2 is needed for the formation of an efficient phagocyte portal in macrophages engulfing apoptotic cells. *J. Immunol.* **182**, 2084-2092 (2009).
32. Guedj, A.S., Kell, A.J., Barnes, M. et al. Preparation, characterization, and safety evaluation of poly(lactide-co-glycolide) nanoparticles for protein delivery into macrophages. *Int. J. Nanomedicine* **10**, 5965-5979 (2015).
33. Tozuka, M., Oka, T., Jounai, N. et al. Efficient antigen delivery to the draining lymph node is key component in the immunogenic pathway of the intradermal vaccine. *J. Dermatol. Sci.* **82**, 38-45 (2016).
34. Goel, G., King, T., Daveson, A.J. et al. Epitope-specific immunotherapy targeting CD4-positive T cells in coeliac disease: two randomized, double-blind, placebo-controlled phase 1 studies. *Lancet Gastroenterol. Hepatol.* **2**, 479-493 (2017).
35. Goel, G., Tye-Din, J.A., Qiao, S.W. et al. Cytokine release and gastrointestinal symptoms after gluten challenge in celiac disease. *Sci. Adv.* **5**, eaaw7756 (2019).

36. Hou, T., Macmillan, H., Chen, Z. et al. An insertion mutant in DQA1\*0501 restores susceptibility to HLA-DM: implications for disease associations. *J. Immunol* **187**, 2442-2452 (2011).

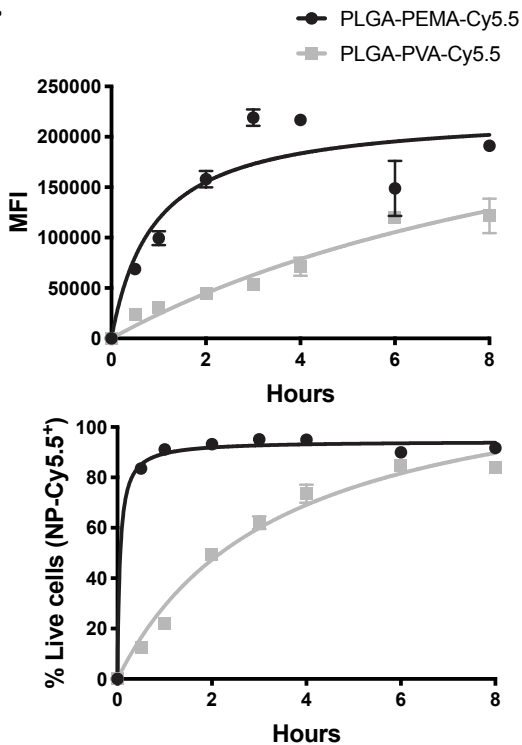
Journal Pre-proof

**Figure 1.**

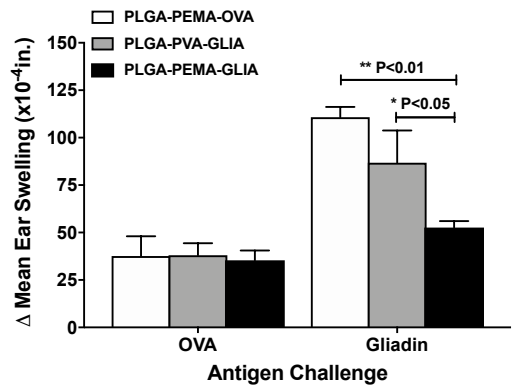
**A.**

Particle	Z-average size (nm)	Zeta potential (mV)	Protein loading ( $\mu\text{g}/\text{mg}$ polymer)
PLGA-PEMA-Cy5.5	405.2 $\pm$ 4.1	-41.2 $\pm$ 0.8	ND
PLGA-PVA-Cy5.5	382.5 $\pm$ 5.6	-16.2 $\pm$ 0.3	ND
PLGA-PEMA-GLIA	695.6 $\pm$ 23	-46.9 $\pm$ 0.6	11.1 $\pm$ 0.6
PLGA-PVA-GLIA	856.9 $\pm$ 54	-18.8 $\pm$ 0.5	9.8 $\pm$ 0.5
PLGA-PEMA-OVA	479.1 $\pm$ 10	-78.8 $\pm$ 18.8	6.2 $\pm$ 0.9
PLGA-PEMA (unloaded)	451.2 $\pm$ 23	-48.7 $\pm$ 5.9	n/a

**B.**



**C.**



**D.**

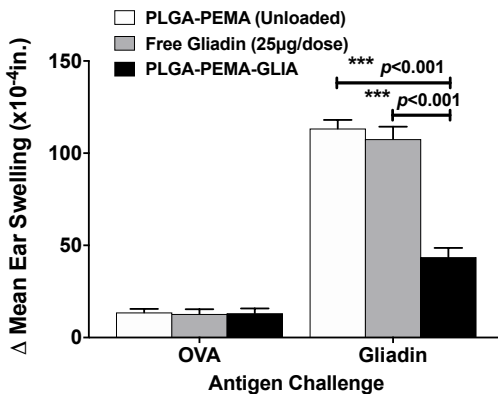
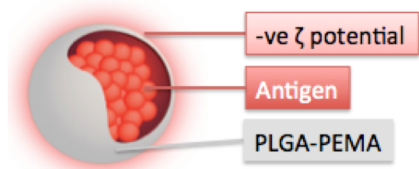


**Figure 2.**

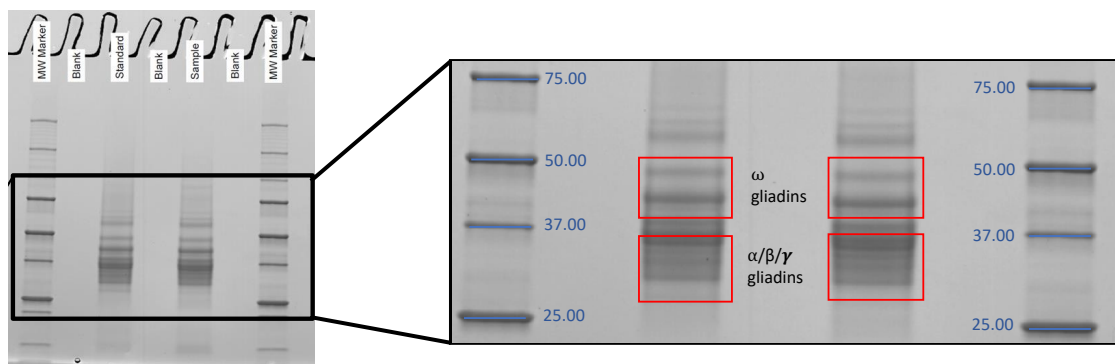
**A.**



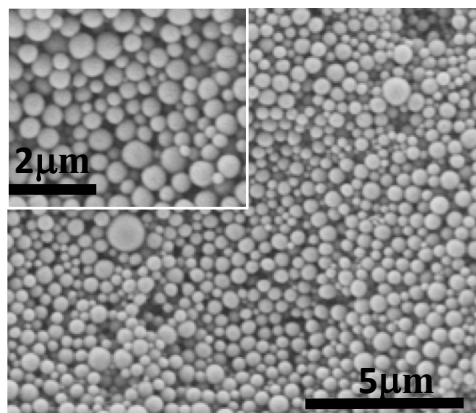
**B.**

Formulation	Z-average size (nm)	zeta potential (mV)	Protein loading ( $\mu\text{g}/\text{mg}$ polymer)	% +ve for surface protein
TIMP-GLIA	$529 \pm 6.4$	$-36.0 \pm 0.5$	$10.8 \pm 1.5$	<1%
TIMP-OVA	$542 \pm 9.7$	$-36.0 \pm 0.3$	$11.6 \pm 0.5$	<1%
TIMP-LYS	$543 \pm 14.8$	$-36.9 \pm 3.9$	$8.9 \pm 1.9$	ND
IMP (unloaded)	$451 \pm 23$	$-48.7 \pm 5.9$	n/a	n/a

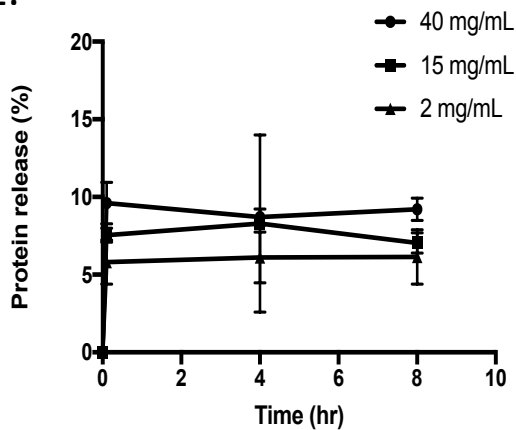
**C.**



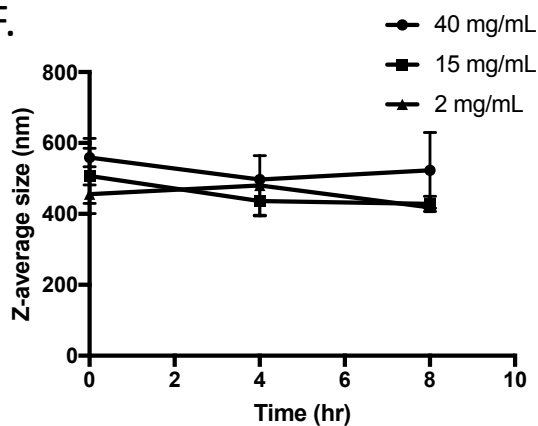
**D.**



**E.**



**F.**



**G.**

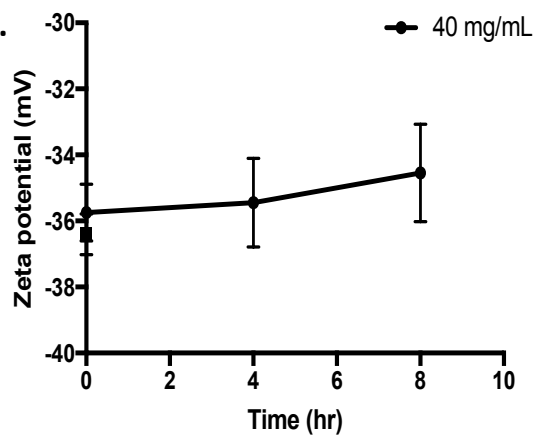




# Figure 3.

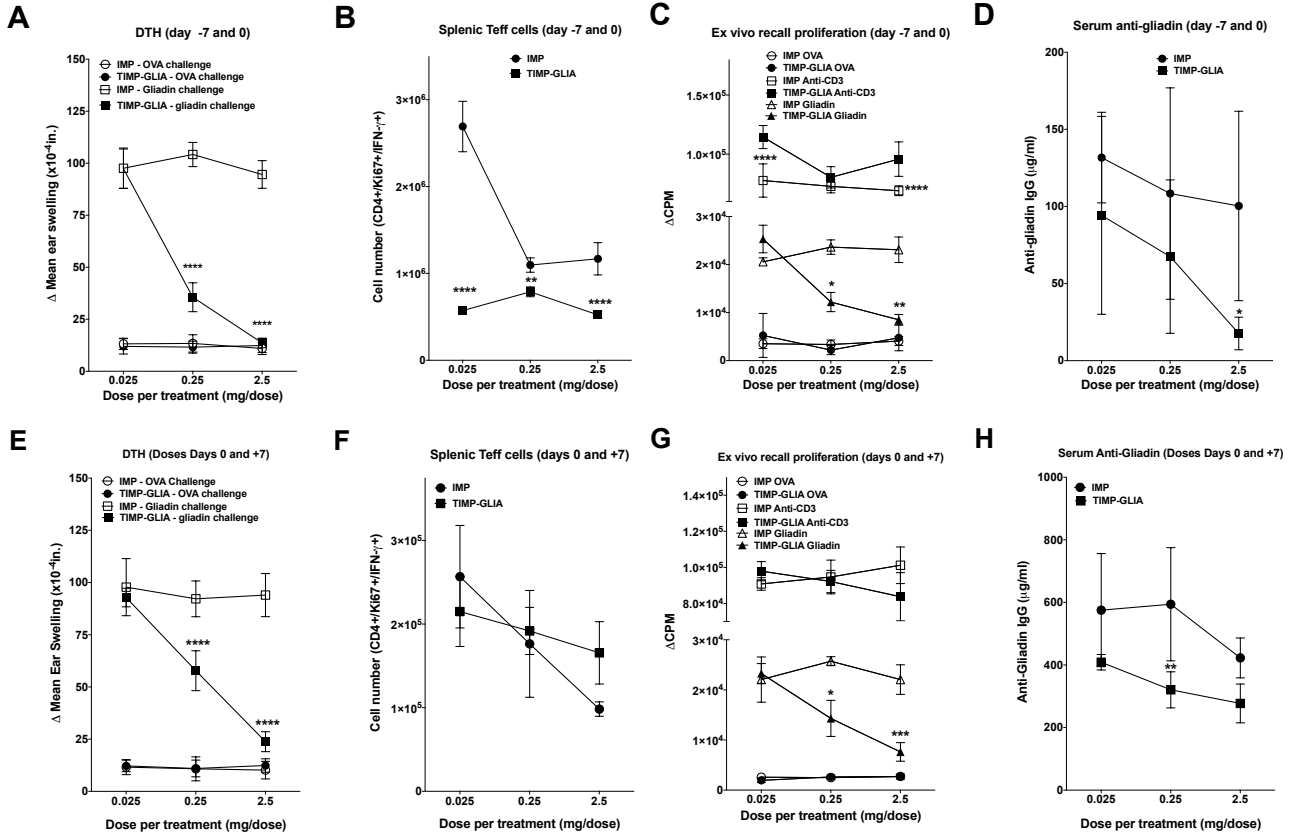


**Figure 4**

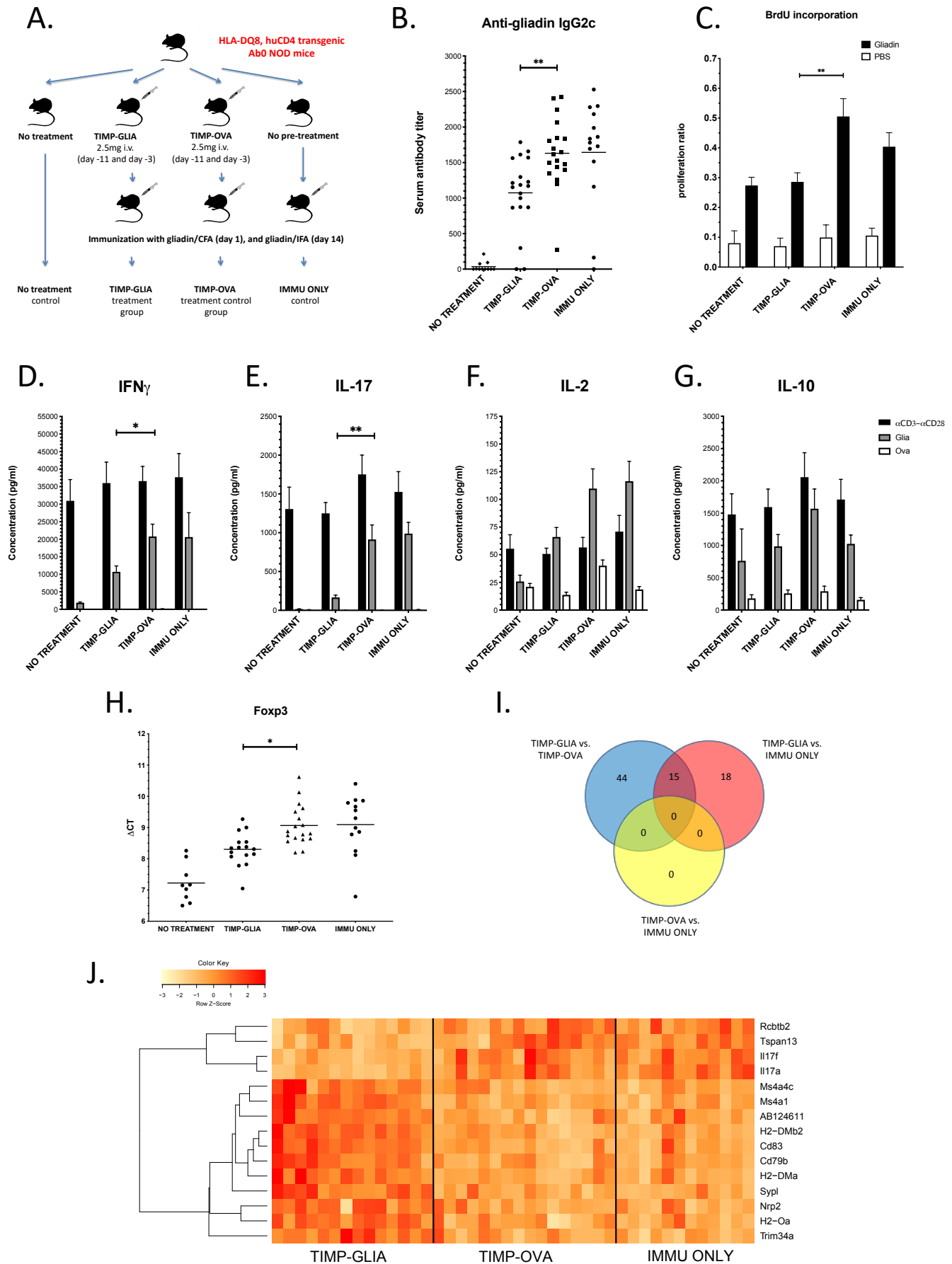


**Figure 5**

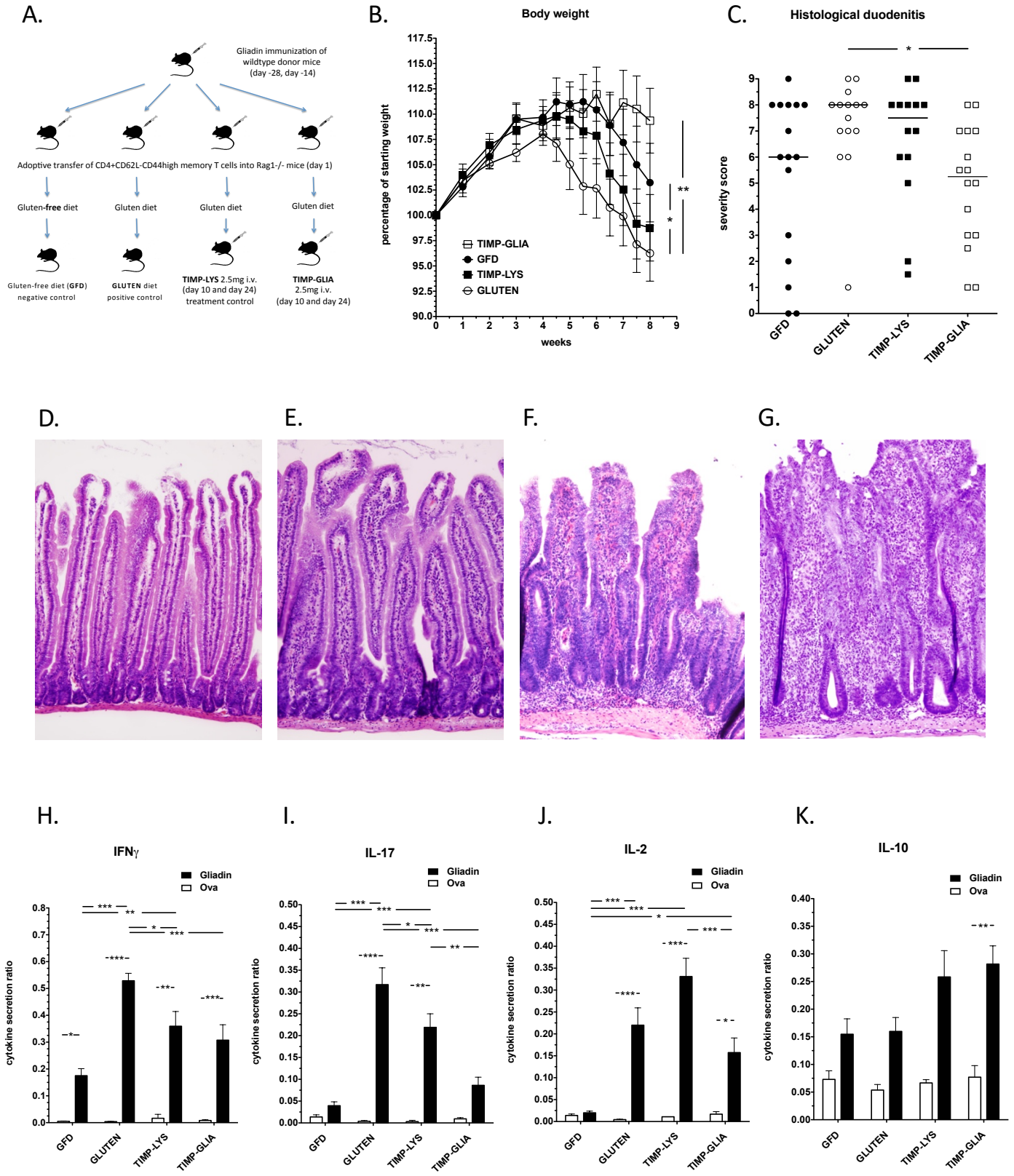
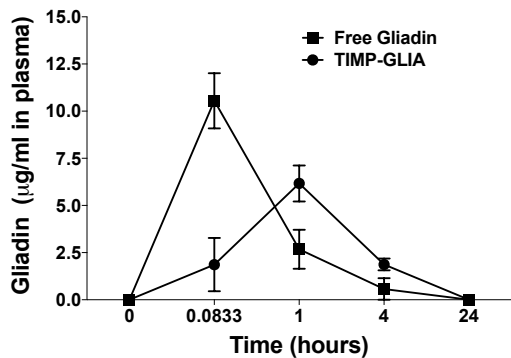
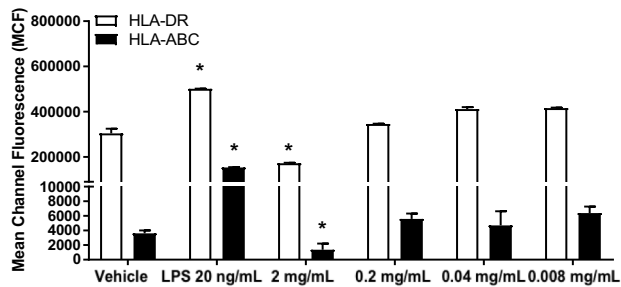


**Figure 6**

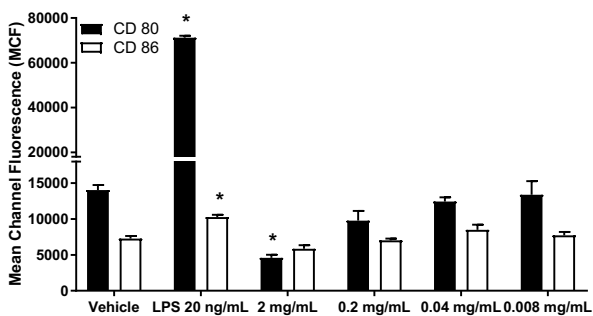
**A.**



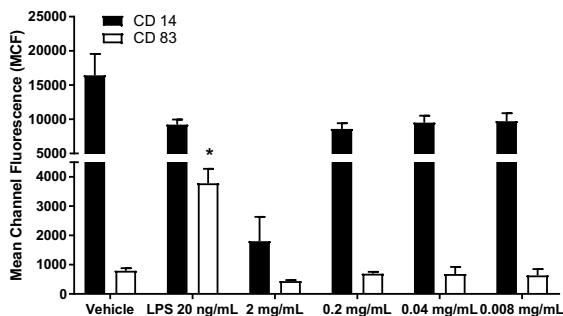
**B.**



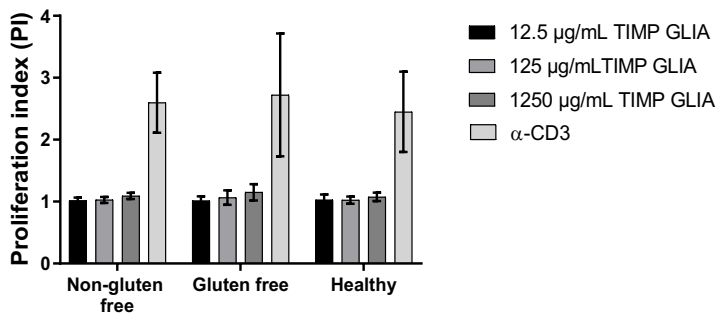
**C.**



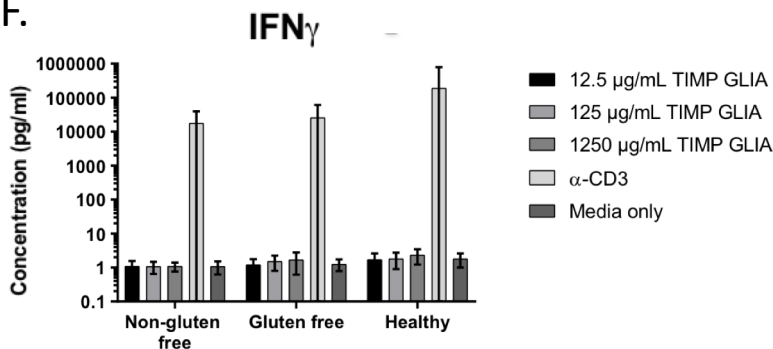
**D.**



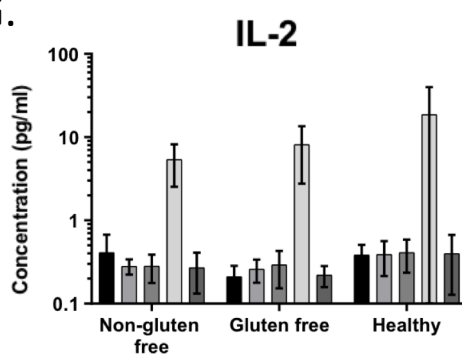
**E.**



**F.**



**G.**



**Supplementary Figure Legends**

**Supplementary figure 1. Western Blot of gliadin preparation** used for production of TIMP-GLIA (duplicates; molecular weight (kDa) of standard proteins indicated).

**Supplementary figure 2. Gating scheme for flow cytometric analysis**, of results presented in figure 3B and F.

**Supplementary figure 3. Cytokine secretion in the gliadin DTH model of draining lymph node or spleen cells restimulated with gliadin *ex vivo*.** C57BL/6 mice (n=5) were treated both on days 0 and 7 with 2.5mg TIMP-GLIA i.v., or unloaded control particles (IMP). Mice were primed with gliadin (100µg/mouse) in CFA on day 0. On day 14, mice were injected with 10ug gliadin into the ear pinna. On day 15, draining lymph node **(A-C)** or spleen cells **(D-F)** were collected, and restimulated in culture medium with anti-CD3 (1µg/ml), OVA, or gliadin (20µg/ml). Cytokines IFN, IL-17 and IL-10 were measured in supernatants. Data are presented as the mean concentration +/- S.E.M. Statistical analyses were performed with t-tests, corrected for multiple testing using the Holm-Sidak method (alpha=0.05; \*p≤0.05, \*\*p≤0.01, \*\*\*p≤0.001).

**Supplementary figure 4. Serum anti-gliadin IgG1 antibody titers in groups of HLA-DQ8 mice**, treated according to figure 4A (n=11-19; ELISA). Statistical analyses were performed using one-way ANOVA and Tukey's multiple comparison test (\*\*\*\*p≤0.0001). Results for comparisons between TIMP-GLIA, TIMP-OVA and IMMUNO ONLY groups were non-significant.

**Supplementary figure 5. Gene expression in gliadin-restimulated spleen cells from transgenic mice expressing celiac disease-associated HLA-DQ8.** Heat map depicting the expression of 77 genes in three groups of HLA-DQ8 mice (TIMP-GLIA, TIMP-OVA, and additional immunized control receiving no treatment with nanoparticles (IMMU ONLY)). Shown is the up- (red) or down-regulation (yellow) of 77 genes differentially expressed in spleen cells restimulated with gliadin, either in comparison between TIMP-GLIA and TIMP-OVA, or between TIMP-GLIA and IMMU ONLY (n=13-16, adjusted p-value  $p \leq 0.05$ ; RNAseq). No genes were differentially expressed between TIMP-OVA and IMMU ONLY. Statistical analyses were performed using edgeR.

**Supplementary figure 6. TIMP-GLIA human biocompatibility *in vitro*.** **A)** Calculation of TIMP-GLIA human equivalent dose (HED) and theoretical plasma concentration, calculated from mouse optimum dose. **B-D)** Effects of TIMP-GLIA on red blood cells and platelets. Hemolysis (**B**) was analyzed by incubation of whole blood with TIMP-GLIA at increasing concentrations vs. Triton X-100 (positive control), PBS (negative control) or nanoparticle formulation buffer (vehicle control), followed by measurement of hemoglobin concentration in supernatants (spectrophotometry). Data expressed as percentage of whole blood hemoglobin concentration. Platelet activation (**C**) and aggregation (**D**) was analyzed by measuring ATP release from platelets (luciferase: luciferin bioluminescence), or sample turbidity, after incubation of platelet rich plasma with TIMP-GLIA at increasing concentrations vs. collagen (positive control) or PBS (negative control). Area under the curve (AUC) was calculated for each sample. **E-G)** Effects of TIMP-GLIA on complement. Production of complement factors Bb (**E**), C4d (**F**) and iC3b (**G**), indicative of complement activation, were analyzed by EIA after incubation plasma with TIMP-GLIA at increasing concentrations vs. cobra venom factor (CVF) and heat aggregated gamma globulin

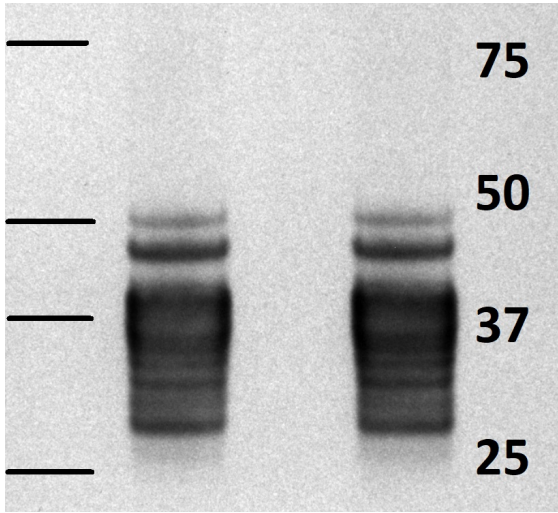
(HAGG) positive controls, or PBS and nanoparticle formulation buffer (saline) negative controls. **H-J**) Effects of TIMP-GLIA on coagulation. Prothrombin time (**H**), activated partial thromboplastin time (**I**) and thrombin time (**J**) was measured after addition to plasma of TIMP-GLIA at increasing concentrations vs. control (saline). Abnormal and normal plasma samples were run as quality controls. All samples were tested in duplicate. Shown is the mean  $\pm$  SD. Statistical analyses were performed using paired t-test, compared to vehicle group (**B-J**; paired t-test, comparison to negative control, \* $p \leq 0.05$ ).

## Supplementary Tables

**Supplementary table 1. Primers used in this study for RNA sequencing.** Design based on the oligonucleotides used by Macosko EZ et al.<sup>20</sup>

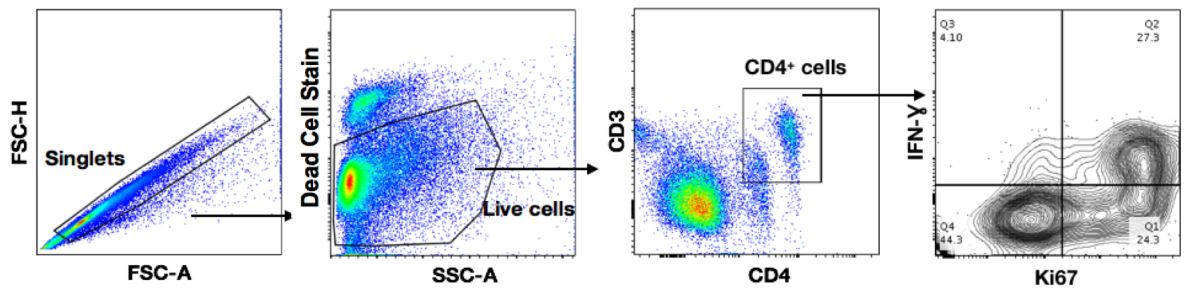
**Supplementary table 2. CD patient and healthy PBMC donor characteristics.** Donors with diagnosed celiac disease were divided into two cohorts, based on their dietary treatment status (gluten free vs. non-gluten free diet). Age, gender, and year of celiac diagnosis were self-reported. HLA-DQ2/-DQ8 status was determined by PCR-SSOP.

# Supplementary figure 1

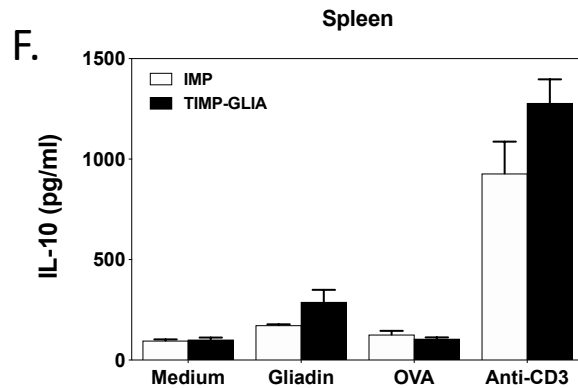
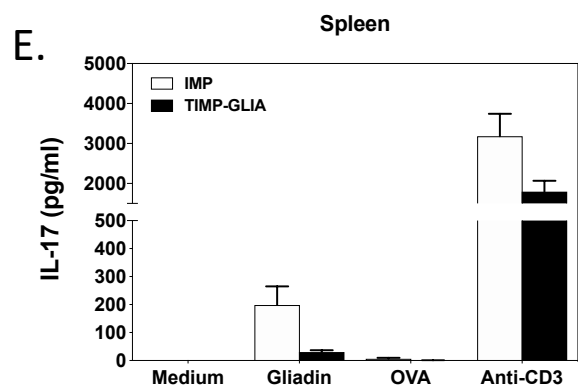
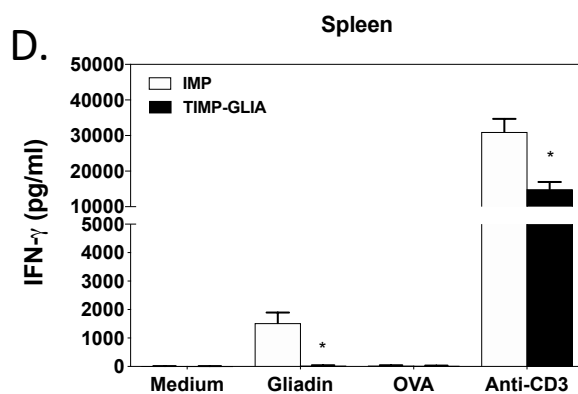
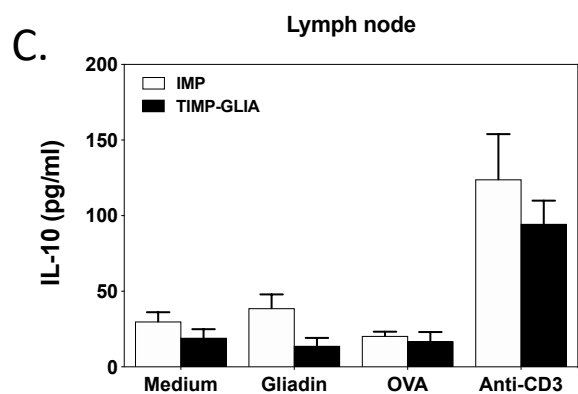
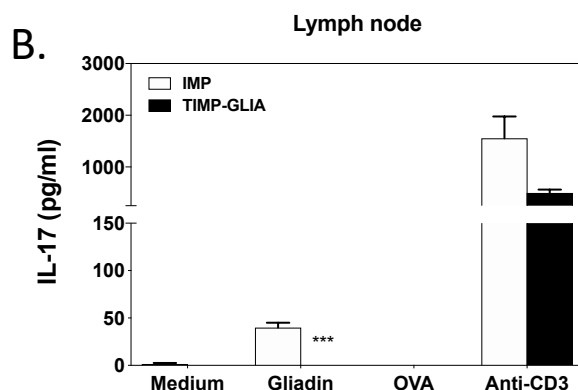
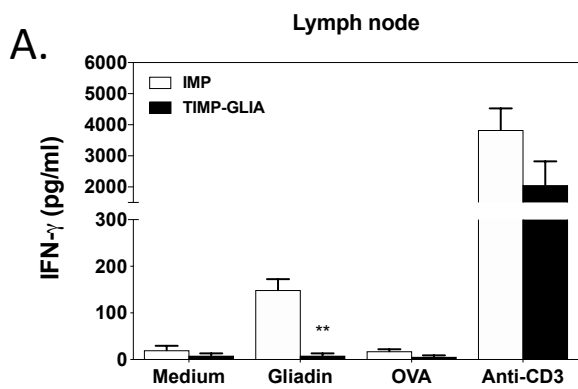




## Supplementary figure 2

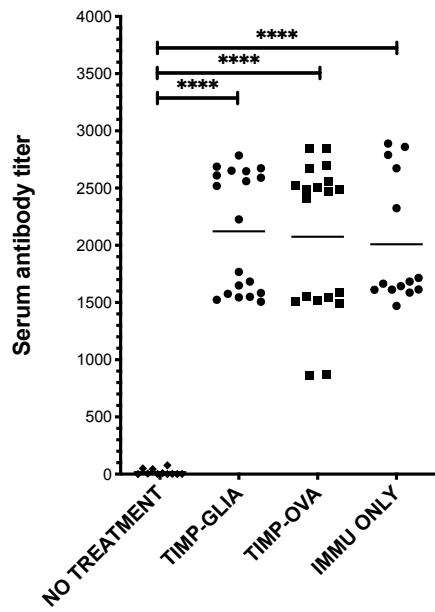


# Supplementary figure 3

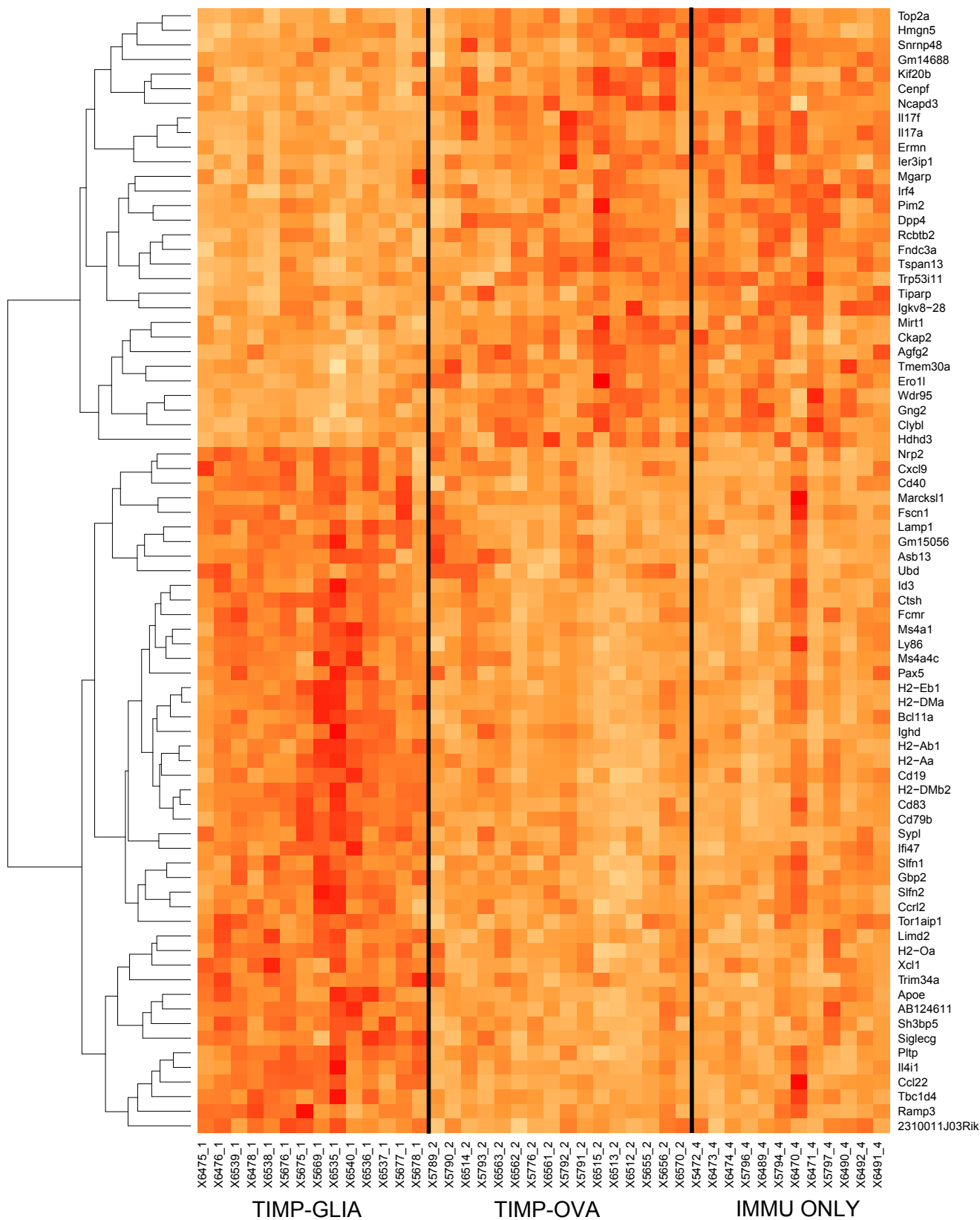
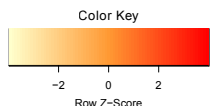


# Supplementary figure 4

## Anti-gliadin IgG1



# Supplementary figure 5



# Supplementary Figure 6

A.

(i) Mouse to human dose translation (modified from NCI National Nanotechnology Laboratory study protocols)

From the experiments displayed in figures 3-5, the optimum dose of TIMP-GLIA in mice is 125 mg/kg.

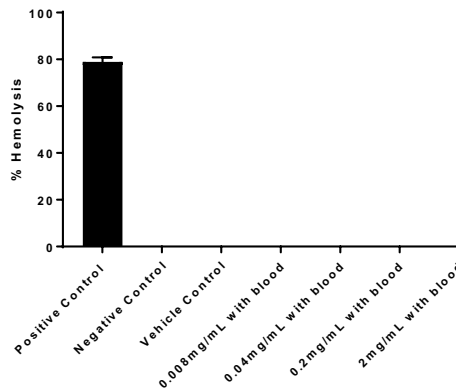
**Human equivalent dose (HED), calculated from mouse optimum dose:  $125 \text{ mg/kg} \div 12.3 = 10.16 \text{ mg/kg}$**

(ii) Translation of HED to *in vitro* dose

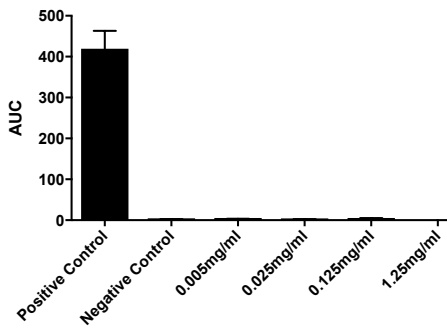
An average person of 70 kg body weight has approximately 5.6 L of blood. Assuming all nanoparticles injected go into the systemic circulation, this provides a rough approximation of the potential maximum nanoparticles concentration in a human. The theoretical plasma concentration, i.e. *in vitro* test concentration is calculated by:

$$\begin{aligned} \text{Theoretical Plasma Concentration} &= \text{Human dose} \div \text{human blood volume} \\ &= (70 \text{ kg} \times 10.16 \text{ mg/kg}) \div 5.6 \text{ L} \\ &= \mathbf{0.127 \text{ mg/mL}} \end{aligned}$$

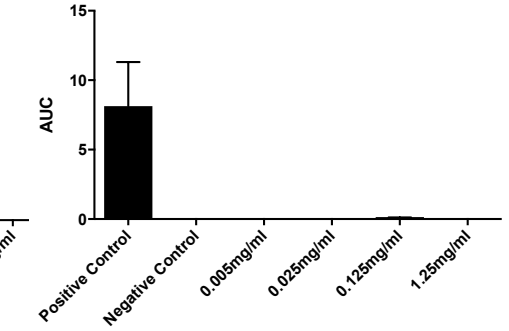
B.



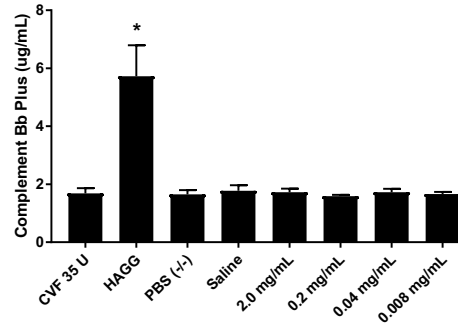
C.



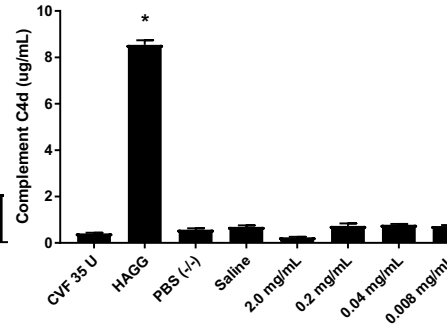
D.



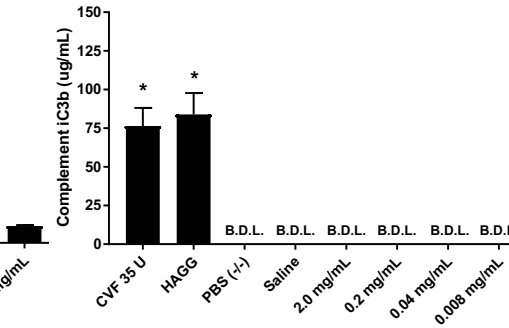
E.



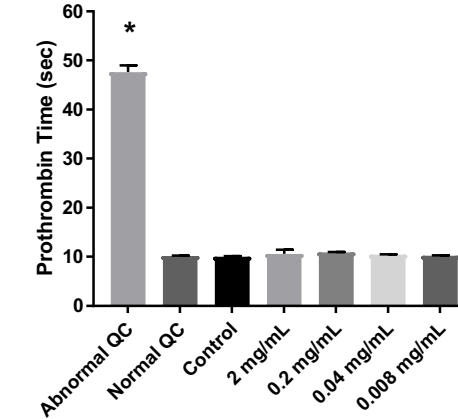
F.



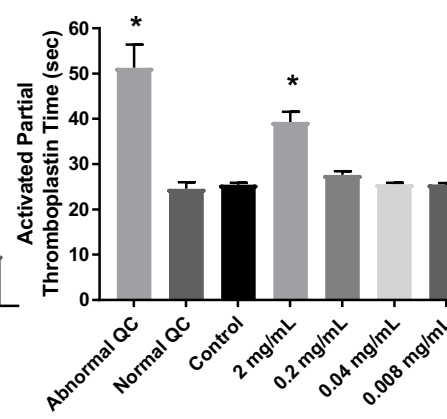
G.



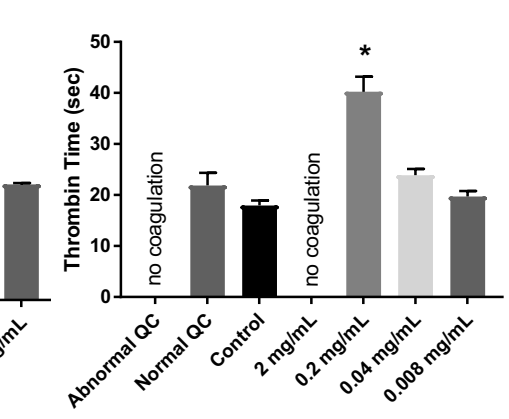
H.



I.



J.



## Supplementary Materials and Methods:

### Nanoparticle size and $\zeta$ potential

Particle size and surface  $\zeta$  potential distributions were obtained using dynamic light scattering on a Zetasizer Nano ZSP (Malvern Instruments, Westborough, MA).

### Macrophage cell culture

Bone marrow from the tibia and femurs of C57BL/6J mice were harvested to obtain a primary population of antigen presenting cells (APCs). Cell media consisted of RPMI 1640 supplemented with glutamine (Life Technologies, Carlsbad, CA), penicillin (100 units/mL), streptomycin (100 mg/mL), 10% heat-inactivated fetal bovine serum (Invitrogen Corporation, Carlsbad, CA). For Bone marrow derived macrophages (BMM $\Phi$ ), the culturing media was further supplemented with 20% L929 conditioned media on days 3 and 6. Unless otherwise mentioned, day-8 BMM $\Phi$  were used for all *in vitro* experiments. The macrophages were removed using versene treatment. The cell numbers and viability were determined using Trypan blue solution and Countess™ Automated Cell Counter (Life Technologies, Carlsbad, CA).

Day-8 BMM $\Phi$ s were seeded in sterile 24-well plates at a concentration of  $1.25 \times 10^5$  cells/well. They were treated with 30  $\mu$ g/mL of PLGA-PEMA-Cy5.5 or PLGA-PVA-Cy5.5 nanoparticle formulations, and incubated at 37°C and 5% CO<sub>2</sub> for up to 8h. Cells were collected at different time points and analyzed by flow cytometry for mean fluorescence intensity, or for percentage of Cy5.5+/DAPI- live cells.

### Nanoparticle surface protein measurement

The surface protein of TIMP-OVA and TIMP-GLIA was measured as previously described.<sup>6</sup> Briefly, 50  $\mu$ g of nanoparticles were incubated with 10  $\mu$ g/mL of anti-OVA-IgG1

(Sigma-Aldrich) or anti-alpha gliadin (clone G12; Biomedal, Sevilla, Spain) for 30 minutes at 4°C, washed, incubated with biotinylated anti-Ig G1 (BD Biosciences, San Jose, CA) followed by washing and incubation with 2.5 µg/mL streptavidin-FITC (eBioscience, San Diego, CA). After a final wash, fluorescence was measured on a BD FACSCanto cytometer (BD Biosciences).

### **Sodium dodecyl sulfate-polyacrylamide gel electrophoresis (SDS-PAGE) of gliadin extract**

SDS-PAGE was carried out using a 4-15% Mini-PROTEAN TGX Stain-Free gel and Tris-glycine running buffer (pH 8.3) containing SDS. The purified gliadin extract (10 µg protein) was dissolved in 15 µL of 0.05M acetic acid, to which Laemmli sample buffer and 2-mercaptoethanol were added. The sample was heated at 95°C for 5 min before allowing to cool to room temperature and loading the sample into the gel. BIO-RAD Precision Plus Protein Unstained Standards (10-250 kD) were used as markers. The running time was 75 min at 110 V. The gel was scanned using a ChemiDoc imaging system (Bio-Rad, Hercules, CA).

### **Gliadin Western Blot**

A solution of gliadin in 50 mM acetic acid (5 mg/ml) was mixed with Bolt LDS Sample Buffer (cat #B0007; Invitrogen) and Bolt Sample Reducing Agent (cat #B0009; Invitrogen), and reduced on a shaker at 70°C for 10 min. A Bolt 4-12% Bis-Tris Plus gel (cat #NW04120BOX; Invitrogen) was loaded with 10 µg of reduced gliadin per well, and ran in MES SDS running buffer (cat #B0002; Invitrogen) at 165V for 45 min. Protein bands were transferred to a nitrocellulose membrane using an iBlot 2NC Regular Stack in an iBlot 2 Gel Transfer Device (Invitrogen) at 20-25V for 7min. After blocking the membrane in

PBS/Tween-20 0.05%/milk 5% for 1 h at RT on a rotating table, the membrane was incubated at 4°C with rabbit anti-gliadin fractionated antiserum (cat #G9144; Sigma-Aldrich), at a dilution of 1/10,000 in PBS/Tween/milk. After washing in PBS/Tween-20 0.05%, the membrane was incubated with goat anti-rabbit IgG-HRP (cat #111-035-144; Jackson ImmunoResearch, Ely, UK) for 1 h at RT, at a dilution of 1/10,000 in PBS/Tween/milk. Protein bands were detected on film, using enhanced chemiluminescence reagent (cat #ORT2251; Perkin Elmer).

### **Electron microscopy**

The surface morphology of TIMP-GLIA was examined using scanning electron microscopy on a FEI/Philips XL30 FEG (FEI, Hillsboro, OR). The cryoprotectant was removed from lyophilized nanoparticles by washing with MilliQ water. A drop of washed particle suspension was placed on carbon adhesive tape, mounted onto an aluminum stub, and dried for at least 2 hr. Samples were sputter coated using gold, and visualized at an accelerating voltage of 5 kV and 7 mm working distance.

### **Burst release assay**

The release of protein from TIMP-GLIA was measured over 8 hr. Three different concentrations (2 mg/mL, 15 mg/mL, and 40 mg/mL) of TIMP-GLIA were dispersed in PBS and incubated at 37 °C. At pre-determined time points, the nanoparticles were centrifuged at 7000 x g for 5 min and the supernatant was collected. The nanoparticles were resuspended in fresh PBS and incubated at 37 °C until the following timepoint. All supernatant samples were stored at -20°C until the experiment was completed. After the final time point, the pellet of nanoparticles was dissolved in DMSO and the total amount of



remaining protein was determined. Protein concentration was determined using the CBQCA assay (Molecular Probes, Waltham, MA).

**Flow cytometry.** For analysis of mouse cells, spleens were collected, dissociated into single cell suspensions, and red blood cells lysed. Splenocytes were cultured *in vitro* in the presence of PMA (50ng/ml) and Ionomycin (500ng/ml) for 2h at 37°C, followed by an additional 2h of culture in the presence of brefeldin A (10µg/ml). At the end of the culture time, cells were collected were subjected to flow cytometric analysis for evaluation of T effector cells (CD3+CD4+CD25+CD44<sup>hi</sup>Foxp3-) and Treg cells (CD3+CD4+CD25<sup>hi</sup>Foxp3+) as follows: Cells were washed three times in PBS, and resuspend with 100µl of LIVE/DEAD® Fixable Aqua Dead Cell Stain Kit (405 nm excitation; Invitrogen, Carlsbad, CA) for 20min on ice, followed by three washes in PBS 5% fetal calf serum. Cells were then resuspended in 100µl of mouse Fc Block (anti-CD16/32; clone 93), diluted 1:100 in 1 PBS 5% FCS, and incubated at 4°C for 20min. The cells were washed three times in PBS 5% FCS, and then stained for 30min in surface staining cocktail of the following antibodies, in a final volume of 100µl: Anti-CD3 (clone 145-2C11), Anti-CD4 (clone GK1.5), Anti-CD25 FITC (clone 7D4), and Anti-CD44 (clone IM7; all antibodies from ThermoFisher Scientific, Grand Island, NY). The cells were then washed three times in PBS, and resuspend 200µl in freshly made Fix/Perm solution (ThermoFisher Scientific), to incubate overnight (or 30min) at 4°C. Following three washes in permeabilization buffer, the cells were resuspended in intracellular staining cocktail containing anti-Foxp3 (clone FJK-16s), anti-IFN-γ (clone XMG1.2), and anti-Ki67 (clone SolA15) in a final volume of 100µl of permeabilization buffer for 30min at 4°C. The cells were then washed three times with permeabilization buffer, and two times with PBS 5% FCS, resuspended in 400µl of PBS 5% FCS, and analyzed by flow cytometry, using the

following gating scheme: Singlets (FSC-A vs. FSC-H) -> Cells (SSC-A vs. FSC-A) -> Live (dead cell stain negative cells) -> CD3/CD4+. Viable cells were analyzed per individual sample using a BD Canto II cytometer (BD Bioscience), and the data analyzed using FloJo Version 9.5.2 software (Tree Star, Ashland, OR).

**Ex vivo recall proliferation (3H-TdR) in the gliadin DTH model.** After testing for DTH, mice were sacrificed, and single cell suspensions from spleens were cultured ( $5 \times 10^5$  cells/well) in the presence of anti-CD3 (1 $\mu$ g/ml), ovalbumin, or gliadin (both 20 $\mu$ g/ml). At 24h post-culture initiation, the wells were pulsed with 1 $\mu$ Ci of 3H-TdR and the cultures harvested at 72h, to measure spleen cell proliferation. Results are expressed as the mean CPM of triplicate cultures.

#### **Serum anti-gliadin antibody ELISA**

To determine the level of anti-gliadin-specific antibody present within serum, 96-well plates were coated with 1 mg gliadin (Sigma-Aldrich) per well. Mouse sera were assayed in serial dilutions. Horseradish peroxidase-labelled anti-mouse IgG (Sigma-Aldrich), IgG1 (Serotec, Oxford, UK) or IgG2c (Bethyl Lab, Montgomery, TX; dilutions 1:10 000 to 1:100 000) was followed by tetramethylbenzidine substrate (Sigma-Aldrich) and spectrophotometric detection at 450 nm. Antibody titres were calculated according to the formula: (OD of sample - OD of blank) x serum dilution.

#### **Ex vivo recall proliferation (BrdU) in the HLA-DQ8 transgenic mouse model**

To measure T cell proliferation, spleen cells from individual mice were cultured in flat-bottom 96-well plates in complete RPMI 1640 at 37°C ( $10^5$ /well; triplicates), and stimulated

with either a combination of anti-CD3 and anti-CD28 antibodies (positive control, 3 µg and 2 µg/ml; clones 145–2C11 and 37.51; eBioscience, San Diego, CA), gliadin or endotoxin-free ovalbumin (negative control, Hyglos, Bernried, Germany; both proteins 20 µg/ml). BrdU was added after 2 days of culture, and cells harvested after 6h incubation. Proliferation was measured using a colorimetric BrdU ELISA kit, following the manufacturer's protocol (Roche, Mannheim, Germany).

### **Mouse cytokine analyses**

IFN- $\gamma$ , IL-17, IL-2 and IL-10 cytokine ELISAs (R&D Systems) were performed with supernatants from spleen cell cultures, restimulated over 72h in 24-well plates (7.5 x 10<sup>6</sup>/well). Cytokine concentrations and ratios between results from individual stimulated samples and corresponding positive control samples were calculated.

**RNA extraction.** RNA was extracted from mouse spleen cells cultured and stimulated for 72h at 37°C in RPMI 1640, and then stored at -20°C in RNAlater (ThermoFisher Scientific), using the RNeasy Mini Kit (Qiagen) and following manufacturer's guidelines. Cells were homogenized with QIAshredder columns (Qiagen). DNA digestion was performed using RNase-free DNase (Qiagen). After extraction, RNA was quantified using a NanoDrop spectrophotometer (ThermoFisher Scientific), or a Qubit 2 fluorometer (Invitrogen) with the Qubit RNA HS Assay Kit (ThermoFisher Scientific). RNA integrity was assessed using the LabChip GXII Touch HT electrophoresis system, with the RNA Assay and the DNA 5K / RNA / Charge Variant Assay LabChip (all PerkinElmer). RNA samples were stored at -70°C.

## RT-qPCR

RT-qPCR reactions were performed using a CFX384 detection system (Bio-Rad, Hercules, CA). Each reaction (final volume of 15  $\mu$ l) contained 7.5  $\mu$ l of 2x RT-PCR buffer, 1.5  $\mu$ l of enzyme mix (both components of the Path-ID™ Multiplex One-Step RT-PCR kit, ThermoFisher Scientific), 25 ng of RNA, 400nM of each primer and 111nM of each hydrolysis probe. 2 optimized, pre-mixed primer/probe sets were used in parallel in the same reaction, a mouse Foxp3-specific set with FAM dye (TaqMan® Gene expression assays, assay ID Mm00475162\_m1, cat# 4331182; Applied Biosystems, Waltham, MA) and a mouse GAPDH-specific set with VIC dye (TaqMan® Gene expression assays, assay ID Mm99999915\_g1, cat# 4331182, Applied Biosystems). Thermal cycling was performed following the kit protocol (Path-ID™ Multiplex One-Step RT-PCR kit, ThermoFisher Scientific). A validation experiment demonstrated that the efficiency of the target and reference gene amplification were approximately equal. All samples were analyzed in triplicates. Additionally, a negative control (RNA-free water), reference control (only GAPDH-specific probe), and target gene control (only Foxp3-specific probe) were included. The level of expression of the Foxp3 target gene was normalized to the level of expression of the GAPDH reference gene in each sample, calculating  $\Delta$ CT values ( $\Delta$ CT = Mean CT Foxp3 – mean CT GAPDH).  $\Delta$ CT values were used for group comparisons.

**RNA-sequencing.** RNA sequencing method was designed based on the Drop-seq protocol.<sup>20</sup> Briefly, 10 ng of RNA was mixed with Indexing Oligonucleotides (Integrated DNA Technologies, Coralville, IA; Supplementary table 1). After 5 minutes of incubation at

ambient temperature the RNA was combined with RT mix, containing 1 x Maxima RT buffer, 1 mM dNTPs, 10 U/ $\mu$ l Maxima H- RTase (all ThermoFisher Scientific), 1 U/ $\mu$ l RNase inhibitor (Lucigen, Middleton, WI) and 2.5  $\mu$ M Template Switch Oligo (Integrated DNA Technologies). Samples were incubated in a T100 thermal cycler (BioRad) for 30 minutes at 22°C and 90 minutes at 42°C. The constructed cDNA was amplified by PCR in a volume of 15  $\mu$ l using 5  $\mu$ l of RT mix as template, 1x HiFi HotStart Readymix (Kapa Biosystems, Wilmington, MA) and 0.8  $\mu$ M SMART PCR primer. The samples were thermocycled in a T100 thermocycler (BioRad) as follows: 95°C 3 min; subsequently four cycles of: 98°C for 20 sec, 65°C for 45 sec, 72°C for 3 min; following 16 cycles of: 98°C for 20 sec, 67°C for 20 sec, 72°C for 3 min; and with the final extension step of 5 min at 72°C. The PCR products were pooled together in sets of 12 samples containing different Indexing Oligos and purified with 0.6X Agencourt AMPure XP Beads (Beckman Coulter, Brea, CA) according to manufacturer's instructions. They were eluted in 10  $\mu$ l of molecular grade water. The 3'-end cDNA fragments for sequencing were prepared using the Nextera XT (Illumina, San Diego, CA) tagmentation reaction with 600 pg of each PCR product serving as an input. The reaction was performed according to manufacturer's instruction, with the exception of the P5 SMART primer that was used instead of S5xx Nextera primer. Each set of 12 samples that was pooled after the PCR reaction was tagmented with a different Nextera N7xx index. Subsequently, the samples were PCR amplified as follows: 95°C for 30 sec; 11 cycles of 95°C for 10 sec, 55°C for 30 sec, 72°C for 30 sec; with the final extension step of 5 min at 72°C. Samples were purified twice using 0.6X and 1.0X Agencourt AMPure Beads (Beckman Coulter) and eluted in 10  $\mu$ l of molecular grade water. The concentration of the libraries was measured using a Qubit 2 fluorometer (Invitrogen) and the Qubit DNA HS Assay Kit (ThermoFisher Scientific). The quality of the sequencing libraries was assessed using the LabChip GXII Touch HT electrophoresis

system (PerkinElmer), with the DNA High Sensitivity Assay (PerkinElmer, Waltham, MA) and the DNA 5K / RNA / Charge Variant Assay LabChip (PerkinElmer). Samples were stored at -70°C. The libraries were sequenced on a Illumina NextSeq 500, with a custom primer (Supplementary table 1) producing read 1 of 20 bp and read 2 (paired end) of 50 bp. Sequencing was performed at the Functional Genomics Unit of the University of Helsinki, Finland.

**Read alignment and generation of Digital Expression Data.** Raw sequence data was filtered to remove reads shorter than 20 bp. Subsequently, the original pipeline suggested in by Macosko EZ et al. for processing of drop-seq data was used.<sup>20</sup> Briefly, reads were additionally filtered to remove polyA tails of length 6 or greater, then aligned to the mouse (mm10) genome using STAR aligner<sup>37</sup>, with default settings. Uniquely mapped reads were grouped according to the 1-12 barcode, and gene transcripts were counted by their Unique Molecular Identifiers (UMIs) to reduce bias emerging from the PCR amplification. Digital expression matrices (DGE) reported the number of transcripts per gene in a given sample (according to the distinct UMI sequences counted). Differentially expressed genes were identified using edgeR.<sup>38</sup>

**Histological Duodenitis Score.** Duodenal samples (2cm length) were fixed in formalin and embedded in paraffin, and sections (6 µm) were stained with hematoxylin and eosin. To identify proliferating cells, longitudinal sections were stained using polyclonal rabbit anti-mouse Ki-67 IgG (dilution 1:500; Bethyl Laboratories), biotinylated goat anti-rabbit IgG, avidin-biotin complex reagent, and diaminobenzidine substrate (all from Vector Laboratories). Hematoxylin was used for counterstaining. The severity of duodenitis was

assessed in a blinded fashion in well-oriented sections and at sites representative for maximal damage, adapting a previously described method.<sup>18</sup> Villus/crypt architecture scores were assigned, as follows: Score 0 (V/C ratio >3.00), 0.5 (2.50– 3.00), 1.0 (2.00– 2.49), 1.5 (1.50–1.99), 2.0 (1.00–1.49), 2.5 (0.50–0.99), 3.0 (<0.5). Villus cellular infiltration was graded, as follows: score 0 (villus lamina propria diameter <0.5 x crypt diameter), 1 (0.5-1x), 2 (1-2x), 3 (>2x). Due to a relatively high baseline of active inflammation in comparison to previous experience, the scores for basal infiltration with neutrophils were adjusted. New scores were based on a statistical distribution analysis including all animals (using 25-percentile, median and 75-percentile as cut-offs): score 0 (normal crypts), 1 [1-7 crypt abscesse(s) per duodenal section], 2 (8-15 crypt abscesses), 3 (>15 crypt abscesses). Each animal was assigned a composite duodenitis score by combining the three separate parameters (maximum score 3 + 3 + 3 = 9).

### **Serum gliadin ELISA**

To determine gliadin serum levels after intravenous injection of soluble gliadin or TIMP-GLIA into C57BL/6 mice, blood samples were collected by retroorbital bleeding from each group of mice at 0 or 5min, 1, 4, or 24h from injection. Gliadin was quantified using a Wheat/Gluten (Gliadin) ELISA Kit (Crystal Chem, Elk Grove Village, Illinois, USA), using the manufacturer's instructions.

### **DC maturation assay**

The effects of TIMP-GLIA on the maturation of human monocyte-derived DC was evaluated *in vitro*, following a published protocol

([https://ncl.cancer.gov/sites/default/files/protocols/NCL\\_Method\\_ITA-14.pdf](https://ncl.cancer.gov/sites/default/files/protocols/NCL_Method_ITA-14.pdf)). Total PBMCs were isolated via Ficoll-Plaque (15ml/tube) from human buffy coats obtained from healthy donors (San Diego Blood Bank, San Diego, CA). Total PBMCs were incubated at  $3 \times 10^6$  cells/ml in DC medium (RPMI-1640 supplemented with 10% fetal bovine serum, 2mM L-glutamine, 25mM HEPES, 100IU/ml penicillin, 100 $\mu$ g/ml streptomycin, 0.1mM MEM NEAA, 1mM sodium pyruvate, and 50 $\mu$ M  $\beta$ -mercaptoethanol) for 1.5h at 37°C to remove non-adherent cells, and the adherent cells were cultured in the presence of DC medium supplemented with IL-4 (50ng/ml) and GM-CSF (100IU/ml) at 37°C for 7 days. On day 7, the non-adherent cells were removed, and the adherent cells were collected for the experimental cultures via incubation with 5mM sterile EDTA in PBS for 15min at room temp. The resulting cells were washed and suspended in fresh DC media (without IL-4 and GM-CSF), and cultured at  $0.5 \times 10^6$  cells/ml in a 24-well plate in the presence of vehicle, LPS (20ng/ml), or TIMP-GLIA (2, 0.2, 0.04 and 0.008 mg/ml) for 48-hours. Following culture, the resultant cells were collected, and the level of HLA-ABC, HLA- DR, CD86, CD80, CD83, and CD14 expression analyzed by flow cytometry.

### **Analysis of hemolytic properties**

The effects of TIMP-GLIA on red blood cells were evaluated *in vitro*, following published protocols ([https://ncl.cancer.gov/sites/default/files/protocols/NCL\\_Method\\_ITA-1.pdf](https://ncl.cancer.gov/sites/default/files/protocols/NCL_Method_ITA-1.pdf)).

Whole blood samples were drawn from healthy donors, and quality assessed by measuring free hemoglobin concentration in plasma. Only samples with a hemoglobin concentration less than 1 mg/ml were used. Whole blood was diluted with PBS to adjust total hemoglobin concentration to  $10 \pm 2$ mg/ml. TIMP-GLIA at increasing doses was incubated with whole blood. Tubes containing TIMP-GLIA only were used as background



control. Triton X-100 at 0.56% was used as positive control, and PBS or saline as negative controls. Inhibition/Enhancement control (IEC) tubes contained 100  $\mu$ L of 5% Triton X-100, 100 $\mu$ L of TIMP-GLIA suspension, 100 $\mu$ L of plasma, whole blood or diluted whole blood, and 600 $\mu$ L PBS. All tubes were placed in a 37°C water bath for 3hrs and 15min. Samples were mixed gently every 30min. Tubes were then centrifugated at 800xg for 15min at room temp. Supernatants were collected, and centrifuged at 18,000xg for 30min at RT to remove TIMP-GLIA from the solution. After addition of Drabkin's solution, cyanmethemoglobin was measured by spectrophotometry at 540nm using a plate reader (Spectra Max i3X, Molecular Devices).

### **Analysis of platelet activation and aggregation**

The effects of TIMP-GLIA on human platelets were evaluated *in vitro*, following published protocols ([https://ncl.cancer.gov/sites/default/files/protocols/NCL\\_Method\\_ITA-2.2.pdf](https://ncl.cancer.gov/sites/default/files/protocols/NCL_Method_ITA-2.2.pdf)). Briefly, platelet rich plasma and platelet poor plasma were prepared from freshly drawn human blood. Plasma from three donors were pooled. Platelet poor plasma was used as background control. Platelet rich plasma was incubated with ChronoLum reagent and test samples, and sample turbidity was measured using an optical Lumi-aggregometer (both from Chrono-Log, Havertown, PA). To measure platelet activation, ATP release from platelets was measured using ChronoLum reagent, based on luciferase:luciferin bioluminescence detection.

### **Analysis of complement activation by EIA**

The effects of TIMP-GLIA on human complement activation *in vitro* were evaluated, following published protocols ([https://ncl.cancer.gov/sites/default/files/protocols/NCL\\_Method\\_ITA-5.2.pdf](https://ncl.cancer.gov/sites/default/files/protocols/NCL_Method_ITA-5.2.pdf)). Human blood was collected from healthy donors using K2-EDTA containing vacutainer tubes. The first 5ml of blood collected was discarded, and the following 5ml blood was collected for the study. Blood was kept at room temperature during the entire processing of the plasma samples. The vacutainer tube was centrifuged (2,500xg; 10min) and the resulting plasma (upper phase) was evaluated for the presence of hemolysis. The resulting plasma (2.5ml) from the vacutainer was carefully transferred to a sterile 15ml conical tube. The assay consisted of four controls; negative (phosphate buffered saline (PBS)), vehicle (saline), positive control (cobra venom factor (CVF) 3.5IU) and a second positive control (Heat Aggregated Gamma Globulin (HAGG)), and testing TIMP-GLIA (0.008, 0.04, 0.2 and 2mg/ml). Samples were prepared in 1.5ml microfuge tubes, containing (100µl of each) veronal buffer, human plasma, and a test sample (CVF 0.35 IU/µl, HAGG (166µM), PBS, saline and TIMP-GLIA (3X final). The assay also included inhibition/enhancement (IEC) controls to determine whether TIMP-GLIA interfered with detection of the complement split product by EIA. The IEC uses the positive control sample after the incubation step. Prior to adding the sample onto the EIA plate, TIMP-GLIA was added to the same final concentrations as used in the study samples. All of the assay samples were vortexed and centrifuged to bring down components (3,000 rpm, 2 minutes at room temp) and incubated in a water bath maintained at 37°C. After the incubation step, aliquots from each sample were further diluted with the corresponding EIA kit sample diluent buffers prior to the addition of the samples to the corresponding EIA detection plates, to assess levels of iC3b, C4d, and Bb (Quidel Corp.; San Diego, CA). After the addition of the stop solution

the optical densities were read using SpectraMax plate reader (450nm for Bb EIA assay and 405nm for iC3b and C4d EIA assay).

### **Coagulation analyses**

The effects of TIMP-GLIA on human plasma coagulation time were evaluated *in vitro*, following published protocols

([https://ncl.cancer.gov/sites/default/files/protocols/NCL\\_Method\\_ITA-12.pdf](https://ncl.cancer.gov/sites/default/files/protocols/NCL_Method_ITA-12.pdf)). Briefly, twenty milliliters of blood were collected from two healthy donors into tubes containing Na-citrate. The blood was immediately centrifuged (2500g; 10 minutes at RT) and the resulting plasma was collected from each tube and maintained at room temp. The resulting plasma layer from each tube was collected and either pooled or kept separate in a sterile 15 mL conical tube maintained at room temp. Aliquots (450 $\mu$ l) of the collected plasma were transferred into 1.5ml Eppendorf tubes. 50 $\mu$ l of TIMP-GLIA (0.008, 0.04, 0.2 and 2mg/ml final concentration), or saline (control), were added to the appropriate tubes, and vortexed. The tubes were incubated at 37°C for 30 minutes, centrifuged (18000g; 5 minutes at 37°C), and the resulting treated plasma supernatants were then tested in triplicate for activated partial thromboplastin time (APTT), prothrombin time (PT), and thrombin time (TT), using a Sysmex AC-600 System (Siemens Healthcare Diagnostics; Tarrytown, NY).

### **Human PBMC proliferation and cytokine secretion assay**

Peripheral blood was collected from healthy donors (n=11), CD donors treated with gluten-free diet (Gluten free) (n=9), and non-treated CD donors (Non-gluten free) (n=11). All donors were between the ages of 18-65, and were HLA-typed for DQ2 and DQ8, using a polymerase chain reaction (PCR)/sequence specific oligonucleotide probes (SSOP) technique on the Luminex platform (Labcorp HLA Laboratory, Burlington, NC; supplementary table 2). PBMC were isolated by density gradient centrifugation. Purified PBMC were stimulated with medium only (negative control), 1 µg/mL anti-CD3 antibody (positive control), or TIMP-GLIA (12.5, 125, or 1250 µg/mL) for 72 h. Proliferation was measured using the CellTiter-Glo Luminescent Cell Viability Assay (Promega, Madison, WI) on the SpectraMax M5 using SoftMax Pro analysis software (Molecular Devices, Downingtown, PA). Proliferation index (PI) values were calculated, relating signals from samples to the signal generated by cells stimulated with medium only. Cytokines in culture supernatants were measured using the MSD Proinflammatory Panel 1 (human) V-Plex kit on the QuickPlex SQ 120, using MSD Discovery WorkBench analysis software (Meso Scale Discovery, Rockville, MD).

#### **Additional references:**

37. Dobin, A., Davis, C.A., Schlesinger, F. et al. STAR: ultrafast universal RNA-seq aligner. *Bioinformatics* **29**, 15-21 (2013).
38. Robinson, M.D., McCarthy, D.J., Smyth, G.K. edgeR: a Bioconductor package for differential expression analysis of digital gene expression data. *Bioinformatics* **26**, 139-140 (2010).

Journal Pre-proof

# Supplementary Table 1

Name	Oligonucleotide sequence
DSbl_001	TTTTTTTAAGCAGTGGTATCAACGCAGAGTACACGTACGTACGTANNNNNNNNNTTTTTTTTTTTTTTTTTT TTTTTTTTT
DSbl_002	TTTTTTTAAGCAGTGGTATCAACGCAGAGTACCGTACGTACGTANNNNNNNNNTTTTTTTTTTTTTTTTTT TTTTTTTTT
DSbl_003	TTTTTTTAAGCAGTGGTATCAACGCAGAGTACGTACGTACGTACNNNNNNNNNTTTTTTTTTTTTTTTTTT TTTTTTTTT
DSbl_004	TTTTTTTAAGCAGTGGTATCAACGCAGAGTACTACGTACGTACGNNNNNNNNNTTTTTTTTTTTTTTTTTT TTTTTTTTT
DSbl_005	TTTTTTTAAGCAGTGGTATCAACGCAGAGTACACGTACGTACGTANNNNNNNNNTTTTTTTTTTTTTTTTTT TTTTTTTTT
DSbl_006	TTTTTTTAAGCAGTGGTATCAACGCAGAGTACCGTAGTACGTACNNNNNNNNNTTTTTTTTTTTTTTTTTT TTTTTTTTT
DSbl_007	TTTTTTTAAGCAGTGGTATCAACGCAGAGTACGTACTACGTACGNNNNNNNNNTTTTTTTTTTTTTTTTTT TTTTTTTTT
DSbl_008	TTTTTTTAAGCAGTGGTATCAACGCAGAGTACTACGACGTACGTNNNNNNNNNTTTTTTTTTTTTTTTTTT TTTTTTTTT
DSbl_009	TTTTTTTAAGCAGTGGTATCAACGCAGAGTACACGTGTACGTACNNNNNNNNNTTTTTTTTTTTTTTTTTT TTTTTTTTT
DSbl_010	TTTTTTTAAGCAGTGGTATCAACGCAGAGTACCGTATACGTACGNNNNNNNNNTTTTTTTTTTTTTTTTTT TTTTTTTTT
DSbl_011	TTTTTTTAAGCAGTGGTATCAACGCAGAGTACGTACACGTACGTNNNNNNNNNTTTTTTTTTTTTTTTTTT TTTTTTTTT
DSbl_012	TTTTTTTAAGCAGTGGTATCAACGCAGAGTACTACGCGTACGTANNNNNNNNNTTTTTTTTTTTTTTTTTT TTTTTTTTT
TSO	AAGCAGTGGTATCAACGCAGAGTGAATrGrGrG
SMART PCR primer	AAGCAGTGGTATCAACGCAGAGT
P5 SMART primer	AATGATACGGCGACCACCGAGATCTACACGCCTGTCCGCGGAAGCAGTGGTATCAACGCAGAGT*A*C
Sequencing read 1	GCCTGTCCGCGGAAGCAGTGGTATCAACGCAGAGTAC

## Supplementary Table 2

Donor #	Cohort	Age	Gender	HLA-DQ2	HLA-DQ8	Year of Celiac Disease Diagnosis
1	Gluten free	50	Female	NEGATIVE	POSITIVE	2005
2	Gluten free	42	Male	POSITIVE	NEGATIVE	2008
3	Gluten free	30	Male	POSITIVE	NEGATIVE	2003
4	Gluten free	43	Female	POSITIVE	NEGATIVE	2011
5	Gluten free	61	Male	POSITIVE	NEGATIVE	2015
6	Gluten free	59	Female	POSITIVE	NEGATIVE	2014
7	Gluten free	71	Female	POSITIVE	POSITIVE	2014
8	Gluten free	28	Female	POSITIVE	NEGATIVE	2016
9	Gluten free	54	Female	POSITIVE	NEGATIVE	2005
10	Gluten free	38	Female	NEGATIVE	POSITIVE	2011
11	Non-Gluten Free	57	Male	POSITIVE	NEGATIVE	2016
14	Non-Gluten Free	52	Female	POSITIVE	NEGATIVE	2006
15	Non-Gluten free	50	Female	POSITIVE	NEGATIVE	2008
17	Non-Gluten Free	33	Female	POSITIVE	NEGATIVE	2012
18	Non-Gluten Free	34	Female	POSITIVE	POSITIVE	2015
19	Non-Gluten Free	64	Female	POSITIVE	NEGATIVE	2004
20	Non-Gluten Free	59	Male	POSITIVE	NEGATIVE	2014
21	Non-Gluten Free	44	Female	POSITIVE	NEGATIVE	2012
22	Non-Gluten Free	48	Female	POSITIVE	NEGATIVE	2014
23	Healthy	60	Male	POSITIVE	NEGATIVE	N/A
24	Healthy	45	Female	POSITIVE	NEGATIVE	N/A
25	Healthy	61	Male	NEGATIVE	NEGATIVE	N/A
26	Healthy	56	Male	NEGATIVE	POSITIVE	N/A
27	Healthy	24	Male	NEGATIVE	POSITIVE	N/A
28	Healthy	55	Female	NEGATIVE	NEGATIVE	N/A
29	Healthy	47	Female	POSITIVE	NEGATIVE	N/A
30	Healthy	37	Male	POSITIVE	NEGATIVE	N/A
31	Healthy	47	Male	POSITIVE	NEGATIVE	N/A
32	Healthy	39	Male	POSITIVE	NEGATIVE	N/A
33	Healthy	34	Male	POSITIVE	NEGATIVE	N/A
34	Healthy	33	Male	POSITIVE	NEGATIVE	N/A

**What you need to know:**

**BACKGROUND AND CONTEXT:** Celiac disease might be cured by restoring T-cell tolerance to gliadin.

**NEW FINDINGS:** In mice with gliadin sensitivity, injection of TIMP-GLIA nanoparticles induced unresponsiveness to gliadin, and reduced markers of inflammation and enteropathy.

**LIMITATIONS:** This study was performed in mice.

**IMPACT:** Gliadin nanoparticles might be developed for treatment of celiac disease.

Lay Summary: We developed nanoparticles that reduce sensitivity to wheat proteins in mice, and might be used to treat celiac disease in patients.